Future changes in the North Atlantic jet stream under climate change

Júlia Casadevall Díaz

Bachelor Thesis on Environmental Science
Universitat de Barcelona,
Facultat de Biologia (Year 2022-23)

Research tutor: Dr Amanda Maycock
University of Leeds, UK
Internal tutor: Dr Miquel Salicrú

ACKNOWLEDGMENTS

Firstly, I would like to thank my project supervisor, Dr Amanda Maycock, for giving me this opportunity as well as for her guidance and support throughout this process.

As well, I would also like to thank Ph.D. student Jacob Perez for his support during the research.

Finally, I'm especially thankful to my parents for supporting me financially and emotionally.

ABSTRACT

Uncertain future changes in the North Atlantic jet stream (NAJ) have been identified as a key source of uncertainty in regional climate projections for Europe. This study aims to investigate the variations of the NAJ by applying a new moment based statistical method for characterising the NAJ and its variability to future projections from five state-of-the-art CMIP6 climate models. This is the first time the method has been used to study future climate and novel insight to changes in jet position, intensity, tilt and width are provided. After verifying the performances of the multi-model ensemble in reconstructing the present day period (1995–2014) in comparison with ERA5 climatology, the future climate variations expected long-term (2080–2099) have also been analysed during the boreal winter (December, January, February) for the shared socio-economic scenario SSP3-7.0. Some CMIP6 models show a significant squeezed, strengthened and extended NAJ to Europe in the seasonal mean. Consistent with the majority of the CMIP6 models, there is hight tendency of a south-west to north-east tilt of the NAJ in future climates, excluding one, that shows the opposite. Just one model predicts a significant poleward shift of the NAJ in winter as a response to global warming. Despite the intermodal differences, there is a consistent reduction in jet latitude and tilt variability, indicating a less variable jet in future rather than an increase in jet variability which has been suggested as a result of Arctic Amplification.

KEYWORDS: Eddy-driven jet; North Atlantic atmospheric circulation; climate dynamics; jet variability; climate change; European climate; CMIP6; ERA5

IDENTIFICATION AND REFLECTION ON THE SUSTAINABLE DEVELOPMENT GOALS (SDGs)

During the past few years, global climate change has become a subject of great concern. In order to achieve the 2030 Agenda for Sustainable Development and its 17 goals it is imperative to take immediate action to combat climate change and its devastating impacts.

This study will inform understanding of the response of the atmosphere to climate change and its role for regional climate change in Europe. Variations in the intensity and position of the North Atlantic jet stream (NAJ) play a critical role in modulating European weather patterns, climate dynamics, transport, commerce, and ecosystems. Note that many recent instances of extreme weather are attributed to jet stream variability, with large societal impacts.

Understanding the potential changes of jet stream under future climate change can have significant implications for a range of Sustainable Development Goals (SDGs).

Investigating the future changes in the NAJ aligns directly with the SDG 13 on Climate action, as it contributes to a better understanding of how climate change can alter the dynamics of atmospheric circulations. Such knowledge it's necessary to develop adaptation strategies to mitigate the adverse effects of climate change on ecosystems, human societies, and economic systems.

As previously mentioned, changes in the NAJ are likely to influence the frequency and intensity of extreme weather events in Europe, including storms, heatwaves, and droughts. Aligned with SDG 11 on Sustainable Cities and Communities, understanding these changes in the weather patterns can help cities and communities prepare for and adapt to these impacts. Cities can become more resilient and sustainable if the projected shifts in the NAJ are integrated into urban planning, infrastructure development, and disaster risk mitigation strategies.

Aligned with the SDG 15 on Life on land, the results of this study, can provide valuable information for scientists to anticipate ecological changes and develop conservation strategies to protect terrestrial habitats and preserve biodiversity, as the NAJ changes can have direct consequences for ecosystems, affecting biodiversity, vegetation patterns and overall ecosystem health.

The NAJ can also influence weather patterns over the ocean affecting sea surface temperatures, oceanic currents, and marine ecosystems. In line with the SDG 14 on Life below water, the analysis of the future variations in the NAJ, can contribute to understanding the consequences for marine habitats, fisheries, and the overall health of marine ecosystems.

Transport efficiency is key to economic development, which is addressed under SDG 9 on Industry, Innovation, and Infrastructure. Changes in the NAJ can alter aircraft flying routes from west to east that benefit from this fast-moving air current, reducing fuel consumption and travel time.

In this study five CMIP6 (Coupled Model Intercomparison Project Phase 6) climate models have been used to project the future changes of the NAJ under climate change scenarios, CMIP6 it is an international effort coordinated by the World Climate Research Programme (WCRP) to evaluate and compare the performance of climate models bringing together scientists and institutions from around the world. This aligns with the SDG 17 on Partnership for the goals as it is focuses on strengthening global partnerships to address global challenges.

In conclusion, this study focused on the future changes of the North Atlantic jet stream under climate change hold great importance for multiple Sustainable Development Goals. Understanding how climate change affects the NAJ and its consequences, can aid in making policies, developing adaptation strategies, and mitigating potential risks necessary for achieving a sustainable and resilient future.

INDEX

1. Introduction

Jet streams are powerful, narrow currents of air that encircle the globe from west to east in the northern and southern hemispheres. Earth has four primary jet streams: two eddy-driven jets (also called polar or midlatitude jets) in mid-latitudes (around 50-60N/S), and two subtropical jets closer to the equator (around 30N/S). The existence of these jets is attributed to different dynamical processes: the subtropical jet forms as a result of angular momentum transport by the thermally direct Hadley circulation (Held and Hou 1980), while the eddy-driven jet forms as a result of eddy momentum flux convergence by atmospheric waves that develop in regions of baroclinic instability (Held, 1975; Rhines, 1975; Panetta, 1993).

In the absence of surface asymmetries and large-scale instability, the jets would encircle the globe, but regional features such as continents, mountains, and patterns of ocean temperatures act to shape the regional jet streams by forcing large-scale wave patterns known as Rossby waves. Rossby waves manifest as successions of alternating regions of low and high pressure around a circle of latitude. These pressure anomalies are known, respectively, as cyclones (low pressure) and anticyclones (high pressure). If a jet stream is present, then the waves can be seen as meanders in the jet, as it snakes to the north and south of the weather systems.

In the northern and southern hemispheres, the mid-latitude baroclinic zone of the atmosphere is associated with a planetary-scale meridional temperature gradient between the equator and the pole. This temperature gradient generates westerly winds that strengthen with height as a consequence of thermal wind balance (Wallace and Hobbs, 2006). Aloft, the strong westerly winds generated by thermal wind balance form mid-latitude jet stream, the speed of which is typically maximised near the tropopause, where the sign of the meridional temperature gradient reverses.

The North Atlantic jet stream (NAJ) is often described as eddy-driven because convergence of momentum flux by eddies is required to support non-zero surface westerlies (Lee and Kim, 2003). The NAJ is highly variable in terms of position and strength, and these variations influences mid-latitude weather systems, with the storm tracks being essentially a surface expression of the jet stream (Hannachi, 2012). Much jet variability can be conceptually viewed as a pulsing in strength or shifting in latitude of jet although other factors such as the meridional tilt of the jet can also be important. Numerous extreme weather and climate events can be attributed to jet stream variability, to name just a few examples: the cold European winter associated with a southward jet shift in 2010 (Cattiaux *et al.,* 2010), the hot European summer associated with a northward jet shift in 2018 (Drouard *et al.,* 2018) and the prolonged California drought of 2011-17, linked to a northward displaced jet (Seager *et al.,* 2015).

Tropical variability has long been understood as a key driver of jet variability, with El Niño/Southern Oscillation (ENSO) events standing as the classic example, but sub seasonal variations such as the Madden-Julian Oscillation have also been shown to exert similar influence on jet variability from week to week in the midlatitudes (Cassou, 2008).

With the mid-latitude meridional temperature gradients being modified by the anthropogenic climate change, the jet streams are expected to adjust in response (Williams, 2016; Vallis *et al.*, 2015; Wollings *et al.,* 2012). In the lower troposphere of the northern hemisphere (NH), the Arctic amplification (AA) is weakening the meridional temperature gradient and with that the NAJ also weakens (Francis, 2012; Haarsma *et al.,* 2013; Francis, 2015). However, in the upper troposphere and lower stratosphere, the meridional temperature gradient is strengthening because of the combined effects of polar lower-stratospheric cooling and tropical upper-tropospheric warming (Lorenz, 2007). This complexity has given rise to a tug-of-war between contrasting effects of the Arctic and Tropics on the mid-latitudes (Cohen *et al.,* 2014).

The theories suggest that as the Arctic warms, changes in the strength and position of the northern hemisphere jet stream will allow blocking events to become more frequent (e.g. Cohen *et al.,* 2014). For example, as the strength of the jet stream is driven by the difference in temperature between the cold air over the Arctic to the north and the milder air to the south, a fast-warming Arctic reduces this temperature difference. This causes a slight drop in zonal winds in the lower troposphere which, in turn, leads to more meandering of the jet stream that allows blocks to form. This means that the cyclones and anticyclones associated with the meanders are more stationary. However, climate models currently suggest that the competing influence of the warming tropics will be more important, consistent with an overall decrease in Northern hemisphere blocking (Kennedy *et al.,* 2016).

Long term jet stream changes are potential indicators of a changing climate (Pena-Ortiz *et al.*, 2013) and several studies have found evidence for a poleward shift in the jet streams and storm tracks (Hartmann *et al.,* 2013). To make projections of the future of the jet under anthropogenic climate change, state-of-the-art climate models are used. While climate models have many known systematic biases, they are based on the basic laws of physics and remain invaluable tools for establishing causality within the complex climate system. In contrast to phenomena such as temperature increases or rising sea levels, interpreting observed long-term changes in jet dynamics is difficult owing to a high level of natural variability of these (Stendel *et al.,* 2021).

2. Objective

The main goal of this study is to investigate the effect of climate change on the North Atlantic eddy-driven jet stream variability.

In this paper, the representation of the North Atlantic eddy-driven jet (NAJ) variability during the NH winter (December-January-February; DJF) in time to future projections of climate derived from state-of-the-art climate models is analysed.

The analysis of the NAJ response to climate change is performed using model output from phase 6 of the Coupled Model Intercomparison Project (CMIP6). The World Climate Research Program's (WCRP) Coupled Model Inter-comparison Project (CMIP) integrations provide an invaluable tool for the wider climate community to analyse present and future climate variability on a wide range of scales and compare model performance. The jet position, tilt and wind speed parameters from a new moment based statistical method for characterising the NAJ, are analysed in order to evaluate the model's response. The models are compared with the ERA5 reanalysis over 1995–2014 to establish any biases in their representation of the NAJ. The NAJ position, tilt and wind speed projections under CMIP6 SPP3-7.0 scenario at the end of the 21st century are evaluated. Finally, projected changes in 850 hPa monthly zonal wind over the North Atlantic region are illustrated. Note that at 850 hPa, the eddy-driven jet is well separated from the subtropical jet, which is strongest in the upper troposphere.

3. Data and methods

The analysis was carried out in the Jupyter Notebook environment, a web-based interactive computing platform for analysing and visualizing data. Different Python libraries has been set up, including NumPy, Matplotlib, Pandas, and SciPy, to facilitate data manipulation, visualization, and statistical analysis. The Python code developed for this project is included in the Appendix II.

3.1. CMIP6 data

Five climate models from CMIP6 have been selected for the analysis; the list of these models along with their ensemble sizes is presented in Table 1. The model output archived from the CMIP6 models is accessible through the Earth System Grid Federation and the UK Centre for Environmental Data Analytics JASMIN cluster. Those models have been used because they provide both daily and monthly zonal wind data and also have multiple ensemble members available so that the distribution of NAJ variability can be well characterised.

The historical simulation covers 1850 to 2014 and uses historical observation-based forcings including concentrations of CO_2 and other long-lived greenhouse gases, volcanic aerosols,

solar forcing, and natural and anthropogenic aerosols, and land use (Eyring *et al.,* 2016). The SSP3–7.0 scenario is chosen to examine the potential NAJ changes in the future. This scenario represents the medium to high end of the possible future pathways and radiative forcing reaches a level of 7.0 W m^{-2} in 2100. On this path, by the end of the century, average temperatures have risen by 3.6C. The last 20 years of simulations (i.e., 1995–2014 and 2080–2099) in both the historical and SSP3-7.0 scenario runs will be evaluated. Note that the four Earth system models (i.e., CanESM5, CNRM-CM6-1 ACCESS-ESM1-5 and UKESM1.0-LL) and one climate model (i.e., IPSL-CM6A-LR) include a representation of the carbon cycle between the atmosphere, ocean, and biosphere when performing the historical and SSP3-7.0 scenario projections. All model's output data are interpolated onto a resolution of 2° × 2°.

Table 1. CMIP6 climate models used in this analysis.

Model	**Historical**	**SSP3-7.0**	**Institute**
IPSL-CM6A-LR	r[1-9]-i1p1f1	r[1-10]-i1p1f1	Institute Pierre Simon Laplace, France
UKESM1-0-LL	r[1-12,16-19]-i1p1f2	r[1-12,16-19]-i1p1f2	Met Office Hadley Centre, United Kingdom
CNRM-CM6-1	r[1-10]-i1p1f2	r[1-6]-i1p1f2	Centre National de Recherches Meteorologiques, France
CanESM5	r[1-7]-i1p1f1	r[1-7]-i1p1f1	Canadian Centre for Climate Modelling and Analysis, Canada
ACCESS-ESM1-5	r[1-8]-i1p1f1	r[2-8]-i1p1f1	Australian Community Climate and Earth System Simulator, Australia

The monthly averaged winter difference between present day and future is represented using a one-dimensional representation of the North Atlantic zonal winds, produced by zonally averaging the winter monthly mean at lower troposphere (850 hPa) zonal winds over the region 0°–60° W, 15°–75° N. Average differences are calculated between December 1995 to February 2014 with the period December 2080 to February 2099. Values over 500 ms^{-1} were screened, because over Greenland the surface is at lower pressure than 850 hPa, so some models do not interpolate parameters 'below' the local surface and this is instead classed as missing data.

3.2. Observational datasets

The climate models are compared with the ERA5 reanalysis dataset. ERA5 provides a numerical description of recent weather and climate by combining models with observations.

Reanalysis data is based upon observed conditions, and a physical model is used to account for any gaps between stations and time steps. The use of the reanalysis dataset allows to quantify the sensitivity of model results to uncertainties in the jet parameters.

The model evaluation is performed with averaged daily ERA-5 zonal wind data over the period 1 December 1995- 28 February 2014 inclusive, giving a total of 20 complete winter seasons (DJF) for analysis. The data is bilinearly interpolated to a 2º x 2º grid. The domain of interest is the North Atlantic and is defined as 15º– 75ºN and 0º– 60ºW, over the pressure level 850 hPa zonal wind (U_{850}).

3.3. Method of moments

3.3.1. Identification of NAJ regions

To identify NAJ regions, a computer vision technique called flooding (Van der Walt et al. 2014) is applied. Full details of the process of the identification methodology is shown by the flow chart in Appendix I Figure A1. To start flooding a seed point is chosen to be the largest maximum in U_{850} field (U_{max}). To reduce the number of maxima found, a minimum value is U_{850}^{*} is chosen to be 8 ms^{-1}. This threshold is based on other studies searching for westerly jet features in 2D wind fields (Woollings *et al.,* 2010; Messori and Caballero 2015; Simpson *et al.*, 2020).

All neighbouring points in field are then checked they meet the same minimum threshold. This results in a binary mask of points that define the NAJ region. On days where multiple maxima occur, the maxima are sorted in descending order starting with the largest. Any maximum within another region is skipped. Finding all the maxima in a 2D field can lead to the identification of small anomalous regions that are not necessarily a part of the NAJ. To account for this, the regions length $L \geq L^{*} = 1661km$ and have longitudinal extent $L_{\lambda} \geq L_{\lambda}^{*} = 20º$. Any regions that do not meet these criteria are removed.

The results are qualitatively insensitive to changes in these parameters. A table of all thresholds is summarised in Table 2. This process is repeated until there are no more maxima remaining for the day. For the ERA5 dataset, the algorithm identifies 75 days with no regions, 3459 days with one region and 169 days with two regions (summarised in Table 3).

Table 2. Values of the threshold parameters used for flooding and removal of unfavourable.

Threshold	Value	Description
U_{850}^{*}	8 ms^{-1}	Seed point and connectivity threshold
L^{*}	1661 km	The minimum length of an NAJ region
L_{λ}^{*}	20º	The minimum longitudinal extent of an NAJ region

Table 3. The frequency of the number of regions.

No. of regions	No. of days
0	62
1	3459
2	180

3.3.2. Moment Equations

Moments are used to describe the shape of a distribution. For the statistics of a 1D distribution, the first and second moments describe its mean and the variance. They have been used for other studies of different geophysical phenomena, such as the polar vortex (Waugh and Randel,1999; Mitchell *et al.,* 2011; Lawrence and Manney, 2018) and tropical cyclone tracks (Nakamura *et al.,* 2009). Moments are used here to characterise dynamical features of the NAJ based on the regions found in the previous section. Three quantities of interest are the intensity, position, and the tilt of the NAJ.

A 2D moment to the $(p + q)$th order for a region is

$$\mu_{pq} = \iint_R \lambda^p \phi^q U_{850}(\lambda, \phi) dA \tag{1}$$

where R is an NAJ region with $dA = r^2 \sin\phi d\lambda d\phi$, where r is the radius of the Earth, λ the longitude and ϕ the latitude. With (1) all metrics can be defined. The strength of the NAJ is measured using the mean on the of an NAJ region,

$$U_{mean} = \frac{\iint_R U_{850}(\lambda,\phi) dA}{\iint_R dA}. \tag{2}$$

The position of the NAJ is defined by the regions centre of mass,

$$\bar{\lambda} = \frac{\mu_{10}}{\mu_{00}}, \ \bar{\phi} = \frac{\mu_{01}}{\mu_{00}}. \tag{3}$$

The same quantity is calculated by Ceppi *et al.* (2014), but for the zonally averaged zonal winds. It should be noted that $\bar{\lambda}$ is sensitive to the choice of domain. Due to the nature of the calculation, a region that spans the full length of the given domain $\bar{\lambda}$ will always lie somewhere close to the centre. This is not true for $\bar{\phi}$, which shows little to no change in its distribution for different longitudinal domains. For these reasons, discussions on $\bar{\lambda}$ are not included. The tilt (α) is computed using the second order moments. This requires μ to be calculated relative to the centre of mass. The centralised moment is defined as

$$\tilde{\mu}_{pq} = \iint_R (\lambda - \bar{\lambda})^p (\phi - \bar{\phi})^q U_{850}(\lambda, \phi) dA \tag{4}$$

Then using this we define α,

$$\alpha = \frac{1}{2}\tan^{-1}\left(\frac{\tilde{\mu}_{11}}{\tilde{\mu}_{20}-\tilde{\mu}_{02}}\right) \quad (5)$$

where negative values indicate a south-west tilt and a positive value a north-east tilt. The metrics outlined here are the most comparable to the JLI and the jet angle index (JAI) of Messori and Caballero (2015). However, higher order moments such as skewness and kurtosis have been used in other studies (Mitchell *et al.,* 2011).

3.4. Analysis metrics

The distribution trends are analysed using a two-sample Kolmogorov-Smirnov test, where the statistical significance is assessed at the 95% confidence level ($p < 0.05$), with the null hypothesis that the two distributions of values are statistically indistinguishable. An overview of the median, mean, standard deviation and skewness is also analysed.

The difference in the mean of two samples is assessed using the two-sided Student's *t* test. To account for autocorrelation in the time series data, the degrees of freedom are reduced using the effective sample size

$$N_{eff} = N\frac{1-r}{1+r} \quad (6)$$

where N_{eff} is the effective sample size, N is the sample size, and r is the lag 1 autocorrelation.

4. **Results**

4.1. Model evaluation

A comparison of the NAJ latitude (phibar) for the models' present-day simulations (colour) with the ERA5 dataset (black) is shown in Figure 1. The winter average phibar in CMIP6 models is higher than in ERA5, as shown in Table 4, with values within 45º-48ºN for models and 44ºN for ERA5. The standard deviation of ERA5 distribution is higher indicating more variability in the jet position. However, CMIP6 models show lower standard deviation, showing more persistent and less variable NAJ position. Note that the ERA5 distribution is highly negative skewed, with large equatorward shifts occurring much more often than large poleward shifts. While the CMIP6 models distributions, excluding ACCESS-ESM1-5, are positive skewed, indicating poleward shifts occur more often.

According to the Kolmogorov Smirnov test (K-S test), see Table 5, with a K-S statistic = 0.041 and a p-value= 0.73, there aren't significant differences at a confidence level of > 95% between CNRM-CM6-1 and ERA5 phibar distributions. While the other CMIP6 models K-S test show

significant differences with ERA5 distributions. Indicating that CNRM-CM6-1 leads to a better representation of the position of the NAJ in comparison to ERA5

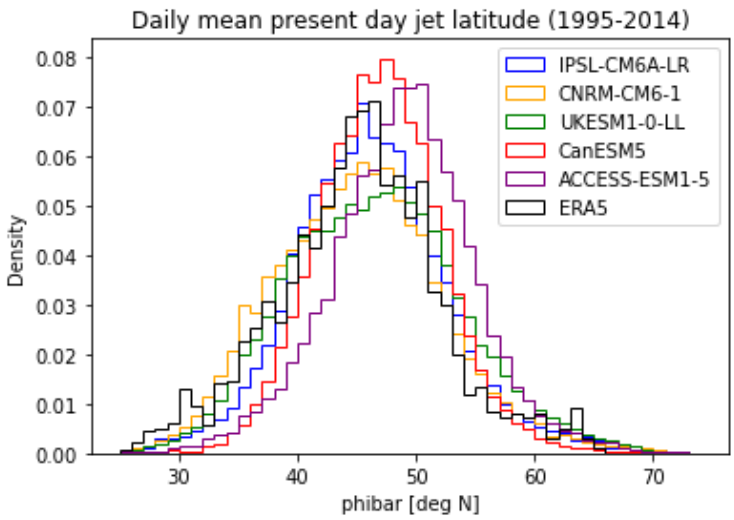

Figure 1. Distribution of the daily DJF North Atlantic jet stream (NAJ) latitude for CMIP6 models and ERA5.

Table 4. phibar median, mean, standard deviation and skewness statistics of CMIP6 and ERA5.

	IPSL-CM6A-LR	CNRM-CM6-1	UKESM1-0-LL	CanESM5	ACCESS-ESM1-5	ERA5
Median	45.92	45.09	46.41	46.95	48.96	45.11
Mean	46.15	45.13	46.49	46.96	48.78	44.13
Standard Deviation	6.62	7.15	7.39	5.24	6.05	9.52
Skweness	0.29	0.29	0.18	0.17	-0.04	-1.94

Table 5. The two-sample Kolmogorov Smirnov Test (K-S test) of each CMIP6 model and ERA5.

	IPSL-CM6A-LR and ERA5	CNRM-CM6-1 and ERA5	UKESM1-0-LL and ERA5	CanESM5 and ERA5	ACCESS-ESM1-5 and ERA5
K-S test (statistic, p-value)	8.32e-02, 4.80e-02	4.14e-02, 7.26e-01	1.02e-01, 4.87e-03	1.58e-01, 4.23e-06	2.65e-01, 2.57e-17

Figure 2 shows a comparison of the frequency of occurrence for the daily present-day winter average NAJ tilt between the CMIP6 models and ERA5. The ERA5 data show a higher peak indicating a narrower distribution (i.e. less variability in jet tilt) than in the CMIP6 models. As shown in Table 6, the mean tilt in CMIP6 and ERA5 are similar. CNRM-CM6-1 is biased towards lower tilt by -1.03º. The standard deviation of all CMIP6 models is higher than ERA5 with CNRM-CM6-1 having a difference of 2.84º. All CMIP6 models and ERA5 distributions are negative skewed, showing instances of highly north-west to south-east tilted jets.

The K-S test for comparison between CMIP6 models and ERA5 shows that all distributions have not significant differences at a confidence level of >95% (p-value<0.05) as shown in

Table 7. That indicates that all CMIP6 models analysed in this study are capable to representing the present-day pattern of the NAJ tilt compared to ERA5.

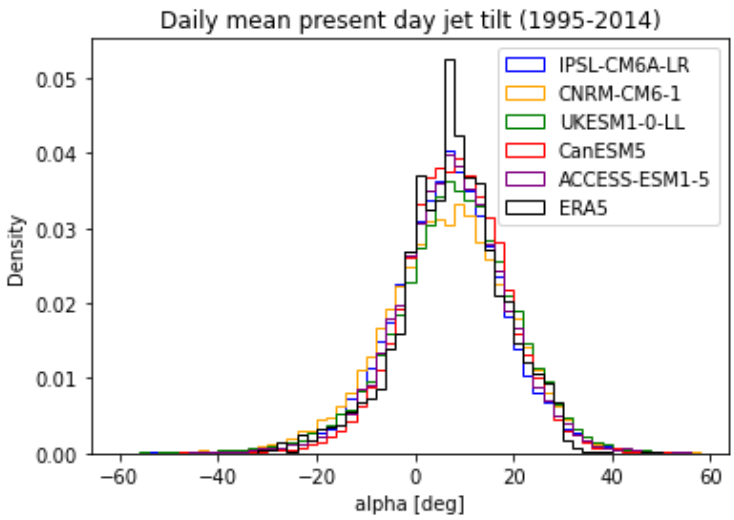

Figure 2. Distribution of the daily DJF North Atlantic jet stream (NAJ) tilt for CMIP6 models and ERA5.

Table 6. alpha median, mean, standard deviation and skewness statistics of each CMIP6 model and ERA5.

	IPSL-CM6A-LR	CNRM-CM6-1	UKESM1-0-LL	CanESM5	ACCESS-ESM1-5	ERA5
Median	6.98	6.97	8.20	8.10	7.57	7.71
Mean	6.72	6.45	7.76	8.06	7.42	7.48
Standard Deviation	11.87	13.47	13.05	10.65	11.75	10.64
Skweness	-0.23	-0.35	-0.47	-0.21	-0.15	-0.29

Table 7. The Two-sample Kolmogorov Smirnov Test (K-S test) of each CMIP6 model and ERA5.

	IPSL-CM6A-LR and ERA5	CNRM-CM6-1 and ERA5	UKESM1-0-LL and ERA5	CanESM5 and ERA5	ACCESS-ESM1-5 and ERA5
K-S test (statistic, p-value)	6.21e-02, 4.79e-01	9.73e-02, 6.42e-02	5.51e-02, 6.21e-01	3.52e-02, 9.75e-01	3.92e-02, 9.37e-01

The comparisons between observed and ERA5 in jet speed (U_{mean}) are shown in Figure 3. There is a clear difference between distributions, where the majority of the CMIP6 models overestimate the mean wind speed. Table 8 confirms this overestimation, with CanESM5 having the highest jet speed, biased 2.35 m/s respect ERA5. All models show lower standard deviation than ERA5, with UKESM1-0-LL biased low by 0.69 m/s. ERA5 wind distribution is highly negative skewed, and all models are positive skewed.

The K-S test, shown in Table 9 indicates that all models' distributions have significant differences at a confidence level of >95% ($p<0.05$) compared to ERA5. None of the CMIP6 models is able to fully simulate the wind speed of the NAJ.

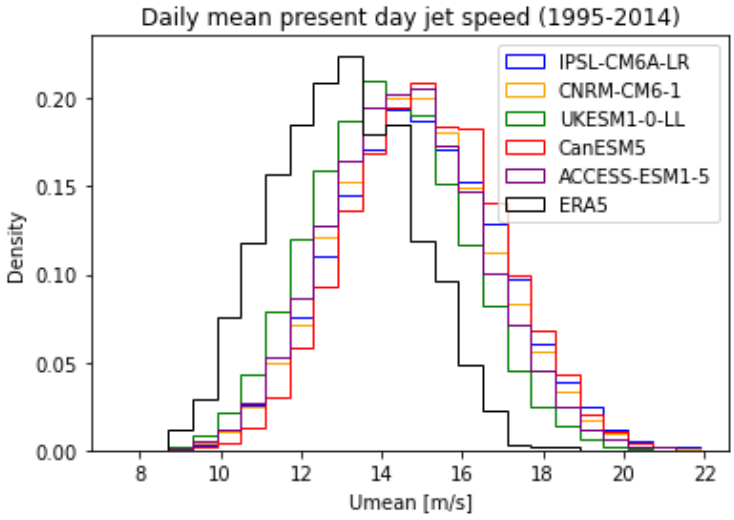

Figure 3. Distribution of the daily DJF North Atlantic jet stream (NAJ) mean wind speed for CMIP6 models and ERA5.

Table 8. Umean median, mean, standard deviation and skewness statistics of each CMIP6 model and ERA5.

	IPSL-CM6A-LR	CNRM-CM6-1	UKESM1-0-LL	CanESM5	ACCESS-ESM1-5	ERA5
Median	14.85	14.75	14.11	15.08	14.58	12.97
Mean	14.92	14.79	14.14	15.12	14.61	12.77
Standard Deviation	2.03	1.95	1.84	1.88	1.90	2.53
Skweness	0.14	0.13	0.12	0.09	0.14	-2.55

Table 9. The Two-sample Kolmogorov Smirnov Test (K-S test) of each CMIP6 model and ERA5.

	IPSL-CM6A-LR and ERA5	CNRM-CM6-1 and ERA5	UKESM1-0-LL and ERA5	CanESM5 and ERA5	ACCESS-ESM1-5 and ERA5
K-S test (statistic, p-value)	3.71e-01, 1.82e-24	3.57e-01, 4.31e-23	2.44e-01, 4.25e-11	4.22e-01, 5.92e-32	3.31e-01, 8.97e-20

The NAJ area-weighted jet speed (U_{mass}) in CMIP6 models and ERA5 are shown in Figure 4. The difference between ERA5 and CMIP6 models is quite visible. Table 10 shows that differences in the mean wind values are quite large, CanESM5 mean U_{mass} value is biased by 0.62×10^{14} km^2*m/s. All models show higher standard deviation than ERA5. ERA5 is positively skewed while all models, excluding UKESM1-0-LL, are negative skewed.

The K-S test, see Table 11, shows that each models shows that all distributions have significant differences with ERA5 at a confidence level of >95% ($p<0.05$). The shapes of the U_{mass} distributions indicate how jet U_{mass} models' values differ between ERA5. There is a big

overestimation of the area-weighted speed across the jet in all models. None of the CMIP6 models is able to fully simulate the area-weighted speed of the jet stream.

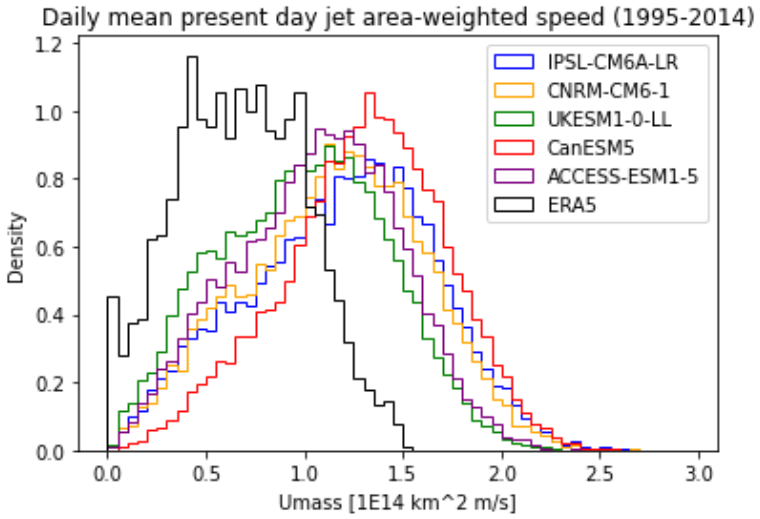

Figure 4. Area-weighted speed across the NAJ distributions of CMIP6 and ERA5.

Table 10. U_{mass} median, mean, standard deviation and skewness statistics of each CMIP6 model and ERA5.

	IPSL-CM6A-LR	CNRM-CM6-1	UKESM1-0-LL	CanESM5	ACCESS-ESM1-5	ERA5
Median	1.22	1.17	1.01	1.32	1.09	0.67
Mean	1.18	1.15	0.99	1.30	1.06	0.67
Standard Deviation	0.47	0.45	0.42	0.41	0.41	0.33
Skweness	-0.14	-0.09	0.01	-0.22	-0.09	0.06

Table 11. The Two-sample Kolmogorov Smirnov Test (K-S test) for U_{mass} of each CMIP6 model and ERA5.

	IPSL-CM6A-LR and ERA5	CNRM-CM6-1 and ERA5	UKESM1-0-LL and ERA5	CanESM5 and ERA5	ACCESS-ESM1-5 and ERA5
K-S test (statistic, p-value)	4.89e-01, 2.39e-09	4.69e-01, 1.39e-08	3.33e-01, 1.48e-04	6.05e-01, 1.54e-14	4.08e-01, 1.12e-06

In summary, the CMIP6 models generally simulate a NAJ that is too poleward, too strong and less variable compared to ERA5, but has a reasonable representation of tilt.

4.2. Future projections of the NAJ under SSP3-7.0

In this section, the response to global warming under SSP3-7.0 by the end of the 21st century is examined in CMIP6 models simulations for the NAJ position, tilt, and strength along with the probability distribution function in the jet parameter time series.

Figure 5 shows the frequency distributions of the daily mean latitude of the NAJ in each CMIP6 model for present day and future periods. All models present similar distributions of the NAJ latitude, with a clear single maximum. There has been extensive work suggesting a poleward

shift of the eddy-driven jet under global warming, which would be evident as a difference in mean between present day and future simulations.

In IPSL-CM6A-LR (Figure 5a), the future trends appear to show higher mean phibar, lower standard deviation, and more positive skewness than in the present-day. However, according to the Student t-test the difference in mean is not significant. The K-S test does indicate the IPSL-CM6A-LR distributions have significant differences, indicating the differences in variability in the jet stream position in the future climate are likely indicative of a climate change impacts. The UKESM1-0-LL phibar distributions has higher variance (see standard deviation from Figure 5b) than the other models, with more points towards the equator, indicating that the NAJ gets stronger more equatorward. The CNRM-CM6-1 future distribution (Figure 5c) is highly skewed, with large poleward shifts occurring much more often than large equatorward shifts. But the mean value for phibar in future climate is lower than present-day. CanESM5 (Figure 5d), show a larger phibar mean, lower standard deviation and no changes in the skewness in future climate. That indicates a more narrowed NAJ with the jet centre located further north. All models, show less standard deviation and positive skewness in the future climate distribution, indicating a more persistent and narrowed NAJ with large poleward shifts occurring more often. None of the models show significant differences between the mean NAJ position in future climate and present-day distributions. According to the K-S test, for all models excluding CNRM-CM6-1 (Figure 5c), the future climate and present-day distributions shape have significant differences. Leading to a different pattern of behaviour of the jet stream position under the future SSP3-7.0 scenario.

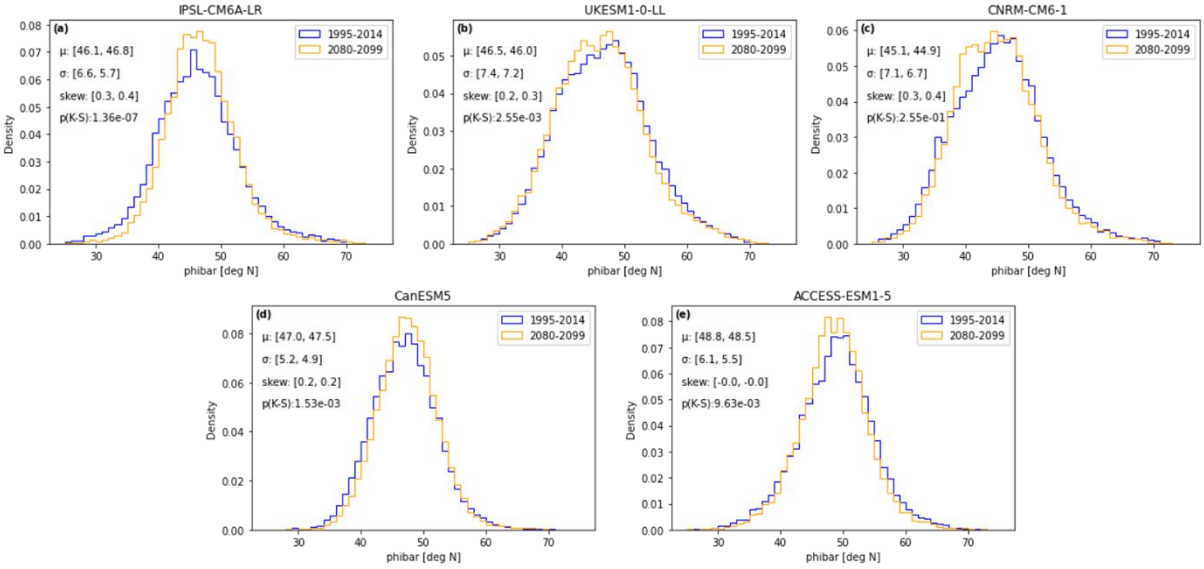

Figure 5. Frequency of occurrence of NAJ latitude in CMIP6 models simulations for present-day and future climate. Summary statistics comparing the two distributions are shown in the inset legends. Bold text indicates a statistically significant difference with a p-value less than 0.05.

Figure 6 shows the frequency distributions of the daily tilt of the NAJ in each CMIP6 model for present day and future periods. All models, excluding CanESM5 (Figure 6d), show a small positive increase in mean tilt in the future, which means a more south-west to north-east tilt. However, the differences are not significant according to a Student's t-test. Both present day and future climate distributions are negative skewed. Although the mean tilt is unchanged, according to the K-S test (Figure 6), all models show significant differences in distributions between present day and future ($p<0.05$). This means that there are other differences in the variability of the tilt of the NAJ by the end of the twenty-first century due to the climate change. These differences are that future projections show a less variability in tilt, as shown in the Figure 6 inset legends, with the standard deviation lower in the future in all models.

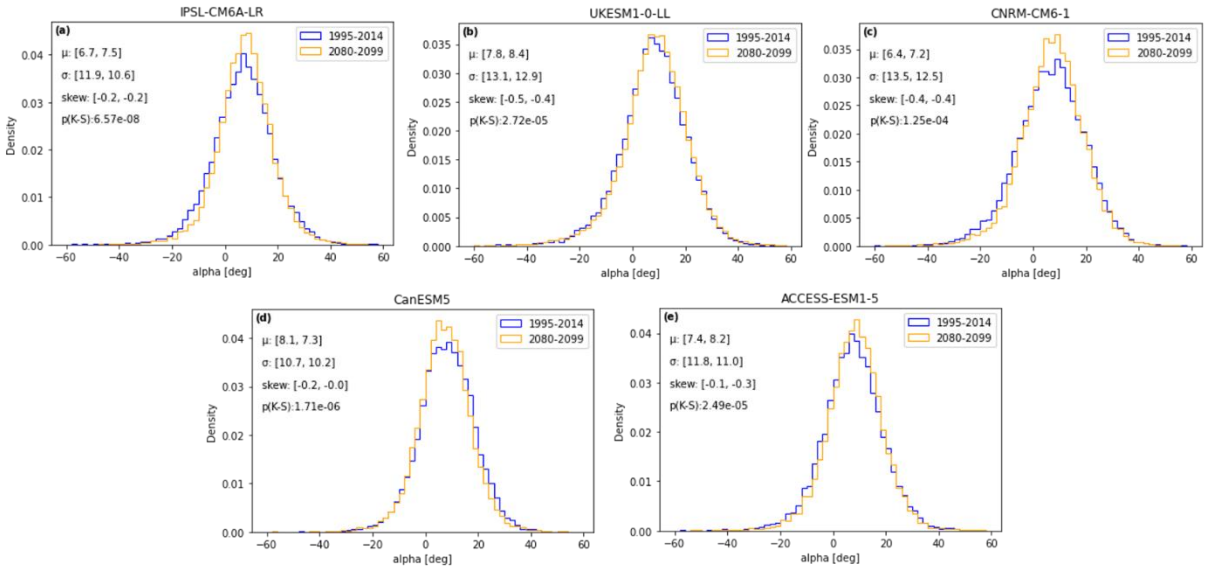

Figure 6. Frequency distributions of the daily winter average tilt of the NAJ relative to the zonal direction of CMIP6 models for present day and future climate periods projections. Summary statistics comparing the two distributions are shown in the inset legends. Bold text indicates a statistically significant difference with a p-value less than 0.05.

The distributions of the average daily zonal wind speed average across the NAJ for present-day and future climate is shown in Figure 7. IPSL-CM6A-LR model future climate distribution (Figure 7a) have a larger U_{mean} value than in present-day. According to the Student t-test the difference is significant. The UKESM1-0-LL (Figure 7b) and CanESM5 (Figure 7d) future climate distributions show interesting results: a significant lower U_{mean} mean, no changes in the standard deviation and a significant K-S test, indicating that both distributions show different behaviour. While CNRM-CM6-1 (Figure 7c) and ACCESS-ESM1-5 (Figure 7e) distributions do not show significant differences in U_{mean} either in the mean or overall shape of the distribution, according to the Student t-test and the K-S test, respectively.

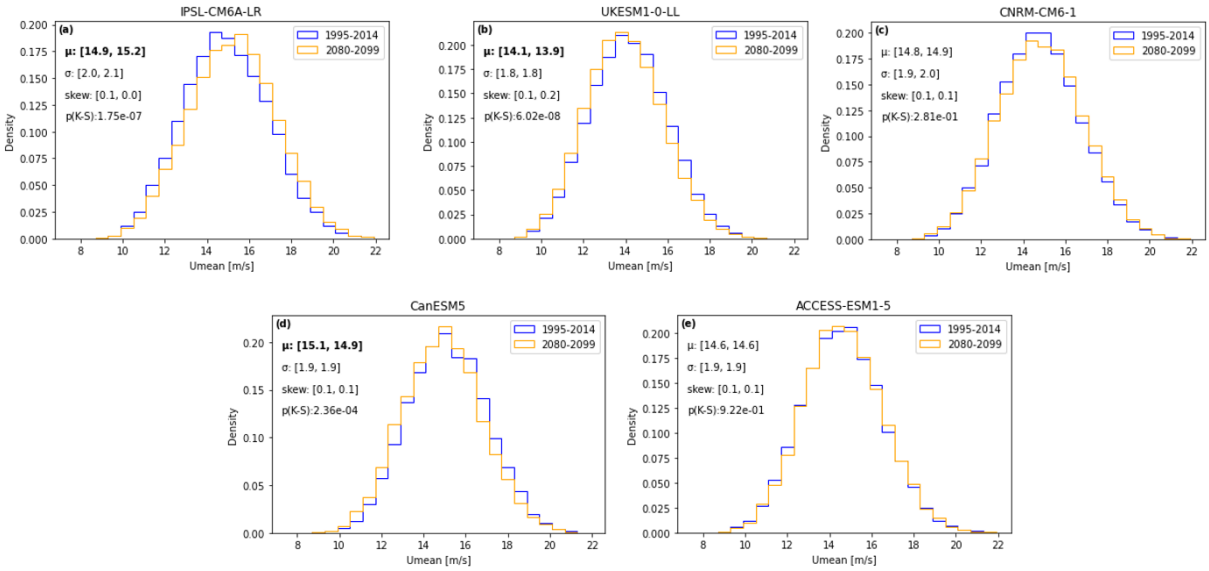

Figure 5. Frequency of occurrence of NAJ U_{mean} in CMIP6 models simulations for present-day and future climate. Summary statistics comparing the two distributions are shown in the inset legends. Bold text indicates a statistically significant difference with a p-value less than 0.05.

The distributions of the average daily area-weighted speed across the NAJ for present-day and future climate are shown in Figure 8. According to the K-S test, only CanESM5 (Figure 8d), IPSL-C6A-LR (Figure 8a) and ACCESS-ESM1 (Figure 8e) show significant differences between present-day and future climate distributions and no significant differences in the mean U_{mass} values of both periods according to the Student t-test. For CNRM-CM6-1 (Figure 8c) and UKESM1-0-LL (Figure 8b), there are not significant differences between present day and future distributions (see K-S test).

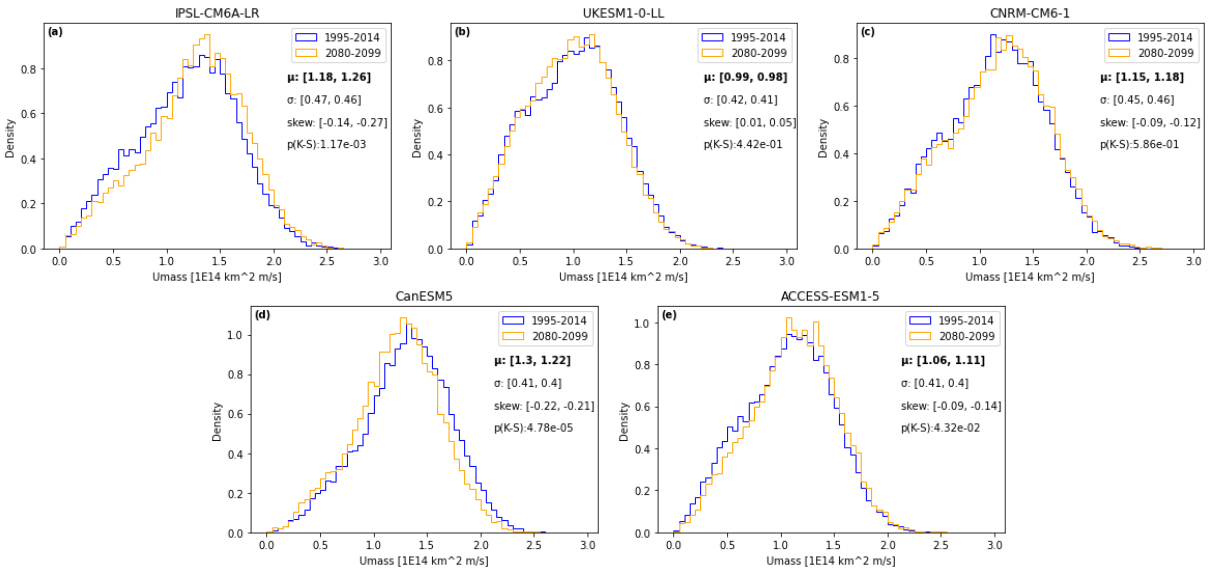

Figure 6. Frequency of occurrence of NAJ U_{mass} in CMIP6 models simulations for present-day and future climate. Summary statistics comparing the two distributions are shown in the inset legends. Bold text indicates a statistically significant difference with a p-value less than 0.05.

None of the models' distributions present a substantial change in the standard deviation. IPSL-CM6A-LR future climate distribution (Figure 8a) shows an increase in the negative skew values.

To assess the impacts of the future climate scenario in the NAJ, the winter mean lower tropospheric zonal wind differences between future and present day across the North Atlantic (NA) region are shown for each model in Figure 9.

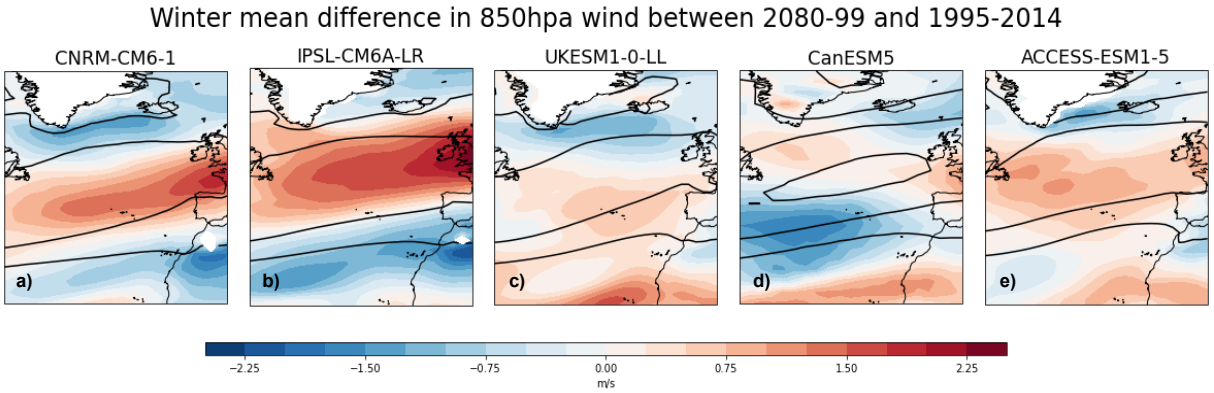

Figure 9. Absolute changes in winter (DJF) 850 hPa monthly mean wind speeds (shaded) for the future climate period (2080–2099) relative to the present day (1995–2014). The contours show the corresponding present-day multimodel mean climatology for each CMIP6 (contour intervals: 5 ms^{-1}).

The term 'jet shift' is referred to the deviation of the jet latitude from a reference state (present day). Such a deviation being positive will mean poleward shift and a negative deviation will correspond to an equatorward shift of the jet.

For CMIP6 models CNRM-CM6-1 (Figure 9a) and IPSL-CM6A-LR (Figure 9b), there is a westerly trend over the North Atlantic region with the strongest climatological winds, representing a strengthening in the core of the NAJ. A notable weakening of the westerly winds is shown in both sides of the NAJ core indicating a narrower jet under future climate change. The strengthening of the NAJ is slightly higher in IPSL-CM6A-LR model (Figure 9b) with a clearly visible poleward shift and extension to Eurasia relative to the present-day state. CNRM-CM6-1 (Figure 9a) also shows a strengthening and extension of the NAJ to Eurasia continent, but little change in the NAJ position. A weak equatorward shift of the NAJ is shown in UKESM1-0-LL (Figure 9c), with higher zonal winds at lower latitudes and a decrease at higher latitudes. CanESM5 (Figure 9d) shows a weak strengthening of the NAJ, shifted poleward in the west NA region, and shifted equatorward at the east region, illustrating a pronounced northwest-southeast tilt. ACCESS-ESM1-5 (Figure 9e) shows a slightly strengthening of the NAJ, but it is weaker than CNRM-CM6-1 (Figure 9a) and IPSL-CM6A-LR (Figure 9b).

5. Discussion

In this study, new reanalysis and climate model datasets (ERA5 and CMIP6) were used to assess the climate model representation of the North Atlantic eddy-driven jet stream. CMIP6 provides the opportunity for a better understanding of the past, present, and future climate. The NAJ's climatology and variability in historical simulations from CMIP6 multimodel archive has been compared with ERA5 reanalysis and CMIP6 SSP3-7.0 scenario future simulations.

CMIP6 models' historical simulations show a less variable and poleward biased NAJ, while ERA5 shows more variability in the NAJ position with large equatorward shifts occurring more often. According to the Kolmogorov–Smirnov test (Table 5), the CNRM-CM6-1 model is the one that has the best representation of present day NAJ latitude.

When it comes to the tilt of the NAJ (Figure 2), CMIP6 models' historical simulations show more variability than observed trends from ERA5. However, all CMIP6 models' historical simulations analysed in this study and ERA5 reanalysis show a significant tendency to a northwest-southeast tilt. According to the K-S test (Table 7), all models are capable to represent the variability of the NAJ tilt.

The majority of the CMIP6 models' historical simulations overestimate the intensity of the NAJ with less variability in the average zonal wind speed values (Figures 3 and 4), indicating a stronger and more persistent NAJ. In comparison, ERA5 reanalysis shows lower and more variable zonal wind speed, indicating a weaker and less persistent NAJ. According to the K-S test (Tables 9 and 11), none of the CMIP6 models' distributions is able to fully represent the intensity of the NAJ.

The future SPP3-7.0 scenario responses in NAJ are not consistent between all CMIP6 models. There are two CMIP6 models (CNRM-CM6-1 and IPSL-CM6A-LR) where the zonal winds are squeezed, strengthened, and extended to Eurasia by the end of the twenty-first century (Figure 9a, b), consistent with Pinto *et al.,* 2007 and Harvey *et al.,* 2020. IPSL-CM6A-LR, also predict a 0.7º poleward shift of the NAJ by the end of the twenty-first century (Figure 6). Davini *et al.* (2014) suggested that the northern jet position tends to be associated with blocking over Europe, so it is possible that the poleward shift predicted in IPSL-CM6A-LR future climate, will be directly linked to the greater frequency of European blocking by the end of the twenty-first century. In addition, a poleward shifted NAJ would lead to a more positive NAO, with warmer, drier summers and milder, wetter winters in western Europe (Hall et al., 2015). In contrast, UKESM1-0-LL predicts a slight strengthening of the zonal winds at lower latitudes, indicating a less narrowed and equatorward shifted NAJ under the same future climate scenario (Figure 9c). CanESM5 shows a weak strengthening of the NAJ, shifted poleward in the west NA region, and shifted equatorward at the east region, predicting a pronounced northwest-

southeast tilt (Figure 9d). Finally, ACCESS-ESM1-5 show a strengthening of the North Atlantic jet but showing no clear shift in DJF by the end of the twenty-first century (Figure 9e).

The fact that U_{mass} shows significant mean changes in the future in all models, but U_{mean} does not, suggests the distribution of winds within the jet area must be altered. In particular, in cases where U_{mass} increases, it suggests there are more frequent occurrences of stronger winds at lower latitudes in the future as compared to present. This could affect the nature of regional extreme events, for example the distribution of severe wind storms (Pinto *et al.,* 2012).

6. Conclusions

This study has investigated the variability in the winter North Atlantic Jet stream in terms of latitude position, tilt and intensity under future climate change. The jet latitude and tilt of CMIP6 models present day simulations are comparable to the reanalysis data (ERA5). However, an overestimation of the wind speed is observed in the majority of the models as compared to ERA5. In summary, the CMIP6 models generally simulate a NAJ that is too poleward, too strong and less variable compared to ERA5, but has a reasonable representation of tilt.

While the five CMIP6 models show differences in their future responses, there are some consistent behaviours that emerge across models. There is a consistent reduction in jet variability in terms of tilt and latitude in all models examined (Figures 5 and 6). This is striking given there is a substantial body of literature suggesting the Northern hemisphere jet is becoming more variable as a result of Arctic Amplification (e.g. Francis and Vavrus, 2015). The results here do not support the jet position becoming more variable in future, but rather that it becomes less variable. The waviness of the midlatitude flow decreases since it is confined to a narrower band of latitudes. This overall decrease in the flow waviness is consistent with results from CMIP5 simulations (Barnes and Polvani 2015; Cattiaux et al. 2016).

The further analysis of mean statistics (jet latitude, tilt and wind speed) of some models under the SPP3-7.0 forcing scenario during the winter, shows a squeezed, strengthened, and extended to Europe jet as a response to global warming. This will affect future weather and climate over Europe, for example by steering storms which are associated with strong winds and heavy precipitation towards Europe (Albern *et al.,* 2021). The eastward extension of the North Atlantic jet stream in response to climate change co-occurs with an eastward extension of the North Atlantic storm track (Harvey *et al.,* 2020). The responses of the jet stream and storm track are of great social and economic interest, with both positive and negative consequences for Europe. On the one hand, the increases in wind speed will result in a higher wind energy production over Northern Europe (Hueging *et al.,* 2013, Moemken *et al.,* 2018). On the other hand, an increase in winter storms over Europe will rise the potential for severe

losses due to storminess and floodings after extreme precipitation events (Leckebusch *et al*., 2007, Pinto *et al.,* 2012, Catto *et al.,* 2019).

A general picture of expected changes cannot be presented since the midlatitude circulation response will depend on the amplitude of several regional processes, in the tropics, at the pole, and in the stratosphere. Intermodal uncertainties are large, highlighting the necessity of performing large ensemble of simulations with different climate models when trying to project midlatitude climate change. Also identifying which factors make the largest contributions to the jet stream uncertainty is an important topic for future research. Further progress on these different aspects will hopefully refine the NAJ response to global warming and consequently the effect on future climate extremes in Europe.

7. References

Albern, N., Voigt, A., & Pinto, J. G. (2021). Tropical cloud-radiative changes contribute to robust climate change-induced jet exit strengthening over Europe during boreal winter. *Environmental Research Letters*, *16*(8), 084041. https://doi.org/10.1088/1748-9326/ac13f0

Barnes, E. A., & Polvani, L. M. (2015). CMIP5 Projections of Arctic Amplification, of the North American/North Atlantic Circulation, and of Their Relationship, *Journal of Climate*, *28*(13), 5254-5271. https://doi.org/10.1175/JCLI-D-14-00589.1

Cassou C. (2008). Intraseasonal interaction between the Madden-Julian Oscillation and the North Atlantic Oscillation. *Nature*, *455*(7212), 523–527. https://doi.org/10.1038/nature07286

Cattiaux, J., Peings, Y., Saint-Martin, D., Trou-Kechout, N., & Vavrus, S. J. (2016). Sinuosity of midlatitude atmospheric flow in a warming world. Geophysical Research Letters, 43(15), 8259–8268. https://doi.org/10.1002/2016gl070309

Cattiaux, J., Vautard, R., Cassou, C., Yiou, P., Masson-Delmotte, V., & Codron, F. (2010). Winter 2010 in Europe: A cold extreme in a warming climate. *Geophysical Research Letters*, *37*(20), n/a. https://doi.org/10.1029/2010gl044613

Catto, J. L., Ackerley, D., Booth, J. R., Champion, A. J., Colle, B. A., Pfahl, S.Pinto, J. G., Quinting, J. F., & Seiler, C. (2019). The Future of Midlatitude Cyclones. *Current Climate Change Reports*, *5*(4), 407–420. https://doi.org/10.1007/s40641-019-00149-4

Ceppi, P., Zelinka, M. D., & Hartmann, D. L. (2014). The response of the Southern Hemispheric eddy-driven jet to future changes in shortwave radiation in CMIP5. *Geophysical Research Letters*, *41*(9), 3244–3250. https://doi.org/10.1002/2014gl060043

Cohen, J., Screen, J. A., Furtado, J. C., Barlow, M., Whittleston, D., Coumou, D., Francis, J. A., Dethloff, K., Entekhabi, D., Overland, J. E., & Jones, J. A. (2014). Recent Arctic amplification and extreme mid-latitude weather. *Nature Geoscience*, *7*(9), 627–637. https://doi.org/10.1038/ngeo2234

Davini, P., Cagnazzo, C., Fogli, P. G., Manzini, E., Gualdi, S., & Navarra, A. (2013). European blocking and Atlantic jet stream variability in the NCEP/NCAR reanalysis and the CMCC-CMS climate model. *Climate Dynamics*, *43*(1–2), 71–85. https://doi.org/10.1007/s00382-013-1873-y

Drouard, M., Kornhuber, K., & Woollings, T. (2019). Disentangling dynamic contributions to summer 2018 anomalous weather over Europe. *Geophysical Research Letters*, 46, 12537– 12546. https://doi.org/10.1029/2019GL084601

Eichelberger, S. J., & Hartmann, D. L. (2007). Zonal Jet Structure and the Leading Mode of Variability, *Journal of Climate*, *20*(20), 5149-5163. https://doi.org/10.1175/JCLI4279.1

Eyring, V., Bony, S., Meehl, G. A., A, C., Senior, Stevens, B., Stouffer, R. J., & Taylor, K. E. (2016). Overview of the Coupled Model Intercomparison Project Phase 6 (CMIP6) experimental design and organization. *Geoscientific Model Development*, *9*(5), 1937–1958. https://doi.org/10.5194/gmd-9-1937-2016

Francis, J. A., & Vavrus, S. J. (2012). Evidence linking Arctic amplification to extreme weather in mid-latitudes. *Geophysical Research Letters*, *39*(6), n/a. https://doi.org/10.1029/2012gl051000

Francis, J. A., & Vavrus, S. J. (2015). Evidence for a wavier jet stream in response to rapid Arctic warming. *Environmental Research Letters*, *10*(1), 014005. https://doi.org/10.1088/1748-9326/10/1/014005

Haarsma, R., Selten, F., & Wanders, N. (2013). Anthropogenic changes of the thermal and zonal flow structure over Western Europe and Eastern North Atlantic in CMIP3 and CMIP5 models. *Climate Dynamics*, *41*(9–10), 2577–2588. https://doi.org/10.1007/s00382-013-1734-8

Hall, R. L., Jones, J. M., Hanna, E., Scaife, A. A., & Erdélyi, R. (2016). Drivers and potential predictability of summer time North Atlantic polar front jet variability. *Climate Dynamics*, *48*(11–12), 3869–3887. https://doi.org/10.1007/s00382-016-3307-0

Hannachi, A., Woollings, T., & Fraedrich, K. (2011). The North Atlantic jet stream: a look at preferred positions, paths and transitions. *Quarterly Journal of the Royal Meteorological Society*, *138*(665), 862–877. https://doi.org/10.1002/qj.959

Harvey, B. J., Cook, P., Shaffrey, L. C., & Schiemann, R. (2020). The response of the northern hemisphere storm tracks and jet streams to climate change in the CMIP3, CMIP5, and CMIP6 climate models. *Journal of Geophysical Research: Atmospheres*, 125, e2020JD032701. https://doi.org/10.1029/2020JD032701

Held, I. M. (1975). Momentum Transport by Quasi-Geostrophic Eddies, *Journal of Atmospheric Sciences*, *32*(7), 1494-1497. https://doi.org/10.1175/1520-0469(1975)032<1494:MTBQGE>2.0.CO;2

Hoskins, B. J., James, I. N., & White, G. H. (1983). The Shape, Propagation and Mean-Flow Interaction of Large-Scale Weather Systems, *Journal of Atmospheric Sciences*, *40*(7), 1595-1612. https://doi.org/10.1175/1520-0469(1983)040<1595:TSPAMF>2.0.CO;2

Hueging, H., Haas, R., Born, K., Jacob, D., & Pinto, J. G. (2013). Regional Changes in Wind Energy Potential over Europe Using Regional Climate Model Ensemble Projections, *Journal of Applied Meteorology and Climatology*, *52*(4), 903-917. https://doi.org/10.1175/JAMC-D-12-086.1

Kennedy, D. P., Parker, T., Woollings, T., Harvey, B. G., & Shaffrey, L. (2016). The response of high-impact blocking weather systems to climate change. Geophysical Research Letters, 43(13), 7250–7258. https://doi.org/10.1002/2016gl069725

Lawrence, Z. D., & Manney, G. L. (2018). Characterizing stratospheric polar vortex variability with computer vision techniques. *Journal of Geophysical Research: Atmospheres*, 123, 1510– 1535. https://doi.org/10.1002/2017JD027556

Leckebusch, G. C., Ulbrich, U., Fröhlich, L., & Pinto, J. G. (2007). Property loss potentials for European midlatitude storms in a changing climate. *Geophysical Research Letters*, *34*(5). https://doi.org/10.1029/2006gl027663

Lee, S., & Kim, H. (2003). The Dynamical Relationship between Subtropical and Eddy-Driven Jets, Journal of the Atmospheric Sciences, 60(12), 1490-1503. https://doi.org/10.1175/1520-0469(2003)060<1490:TDRBSA>2.0.CO;2

Lorenz, D. H., & DeWeaver, E. (2007). Tropopause height and zonal wind response to global warming in the IPCC scenario integrations. *Journal of Geophysical Research*, *112*(D10). https://doi.org/10.1029/2006jd008087

Messori, G., & Caballero, R. (2015). On double Rossby wave breaking in the North Atlantic. *Journal of Geophysical Research: Atmospheres*, *120*(21), 11,129-11,150. https://doi.org/10.1002/2015jd023854

Mitchell, D. J. B., Charlton-Perez, A., & Gray, L. J. (2011). Characterizing the Variability and Extremes of the Stratospheric Polar Vortices Using 2D Moment Analysis. *Journal of the Atmospheric Sciences*, *68*(6), 1194–1213. https://doi.org/10.1175/2010jas3555.1

Moemken, J., Reyers, M., Feldmann, H., & Pinto, J. G. (2018). Future changes of wind speed and wind energy potentials in EURO-CORDEX ensemble simulations. *Journal of Geophysical Research: Atmospheres*, 123, 6373– 6389. https://doi.org/10.1029/2018JD028473

Monahan, A. H., Fyfe, J. C., Ambaum, M. H. P., Stephenson, D. B., & North, G. R. (2009). Empirical Orthogonal Functions: The Medium is the Message. *Journal of Climate*, *22*(24), 6501–6514. https://doi.org/10.1175/2009jcli3062.1

Panetta, R. L. (1993). Zonal Jets in Wide Baroclinically Unstable Regions: Persistence and Scale Selection, *Journal of Atmospheric Sciences*, *50*(14), 2073-2106. https://doi.org/10.1175/1520-0469(1993)050<2073:ZJIWBU>2.0.CO;2

Panetta, R. L., & Held, I. M. (1988). Baroclinic Eddy Fluxes in a One-Dimensional Model of Quasi-geostrophic Turbulence, *Journal of Atmospheric Sciences*, *45*(22), 3354-3365. https://doi.org/10.1175/1520-0469(1988)045<3354:BEFIAO>2.0.CO;2

Peña-Ortiz, C., Gallego, D., Ribera, P., Ordoñez, P., & Del Carmen Alvarez-Castro, M. (2013). Observed trends in the global jet stream characteristics during the second half of the 20th century. *Journal of Geophysical Research: Atmospheres*, *118*(7), 2702–2713. https://doi.org/10.1002/jgrd.50305

Pinto, J. G., Karremann, M. K., Born, K., Della-Marta, P. M., & Klawa, M. (2012). Loss potentials associated with European windstorms under future climate conditions. *Climate Research*, *54*(1), 1–20. https://doi.org/10.3354/cr01111

Pinto, J.G., Ulbrich, U., Leckebusch, G.C. *et al.* Changes in storm track and cyclone activity in three SRES ensemble experiments with the ECHAM5/MPI-OM1 GCM. *Clim Dyn* **29**, 195–210 (2007). https://doi.org/10.1007/s00382-007-0230-4

Rhines, P. B. (1975). Waves and turbulence on a beta-plane. *Journal of Fluid Mechanics*, *69*(3), 417–443. https://doi.org/10.1017/s0022112075001504

Seager, R., Hoerling, M. P., Schubert, S. D., Wang, H., Lyon, B., Kumar, A., Nakamura, J. A., & Henderson, N. (2015). Causes of the 2011–14 California Drought*. *Journal of Climate*, *28*(18), 6997–7024. https://doi.org/10.1175/jcli-d-14-00860.1

Simpson, I. R., Bacmeister, J. T., Neale, R., Hannay, C., Gettelman, A., Garcia, R. R., Lauritzen, P. H., Marsh, D. R., Mills, M. J., Medeiros, B., & Richter, J. H. (2020). An Evaluation of the Large-Scale Atmospheric Circulation and Its Variability in CESM2 and Other CMIP Models. *Journal of Geophysical Research: Atmospheres*, *125*(13). https://doi.org/10.1029/2020jd032835

Stendel, M., Francis, J. A., White, R. H., Williams, P., & Woollings, T. (2021b). The jet stream and climate change. In Elsevier eBooks (pp. 327–357). https://doi.org/10.1016/b978-0-12-821575-3.00015-3

Vallis, G. K., Zurita-Gotor, P., Cairns, C. W., & Kidston, J. (2015). Response of the large-scale structure of the atmosphere to global warming. *Quarterly Journal of the Royal Meteorological Society*, *141*(690), 1479–1501. https://doi.org/10.1002/qj.2456

Van Der Walt, S., Schönberger, J. L., Nunez-Iglesias, J., Boulogne, F., Warner, J. D., Yager, N., Gouillart, E., & Yu, T. (2014). scikit-image: image processing in Python. *PeerJ*, *2*, e453. https://doi.org/10.7717/peerj.453

Wallace, J. L., & Hobbs, P. V. (2006). Atmospheric Dynamics. In Atmospheric Science. An Introductory Survey. https://doi.org/10.1016/b978-0-12-732951-2.50012-0

Waugh, D. W., & Randel, W. J. (1999). Climatology of Arctic and Antarctic Polar Vortices Using Elliptical Diagnostics, *Journal of the Atmospheric Sciences*, *56*(11), 1594-1613. https://doi.org/10.1175/1520-0469(1999)056<1594:COAAAP>2.0.CO;2

Williams, P. (2016). Transatlantic flight times and climate change. *Environmental Research Letters*, *11*(2), 024008. https://doi.org/10.1088/1748-9326/11/2/024008

Woollings, T., & Blackburn, M. (2012). The North Atlantic Jet Stream under Climate Change and Its Relation to the NAO and EA Patterns. *Journal of Climate*, *25*(3), 886–902. https://doi.org/10.1175/jcli-d-11-00087.1

Woollings, T., Barnes, E. A., Hoskins, B. J., Kwon, Y., Lee, R. J., Li, C., Madonna, E., McGraw, M. C., Parker, T., Rodrigues, R. R., Spensberger, C., & Williams, K. L. (2017). Daily to Decadal Modulation of Jet Variability. *Journal of Climate*, *31*(4), 1297–1314. https://doi.org/10.1175/jcli-d-17-0286.1

Woollings, T., Hannachi, A., & Hoskins, B. J. (2010). Variability of the North Atlantic eddy-driven jet stream. *Quarterly Journal of the Royal Meteorological Society*, *136*(649), 856–868. https://doi.org/10.1002/qj.625

APPENDIX I. Flow chart for finding the NAJ regions

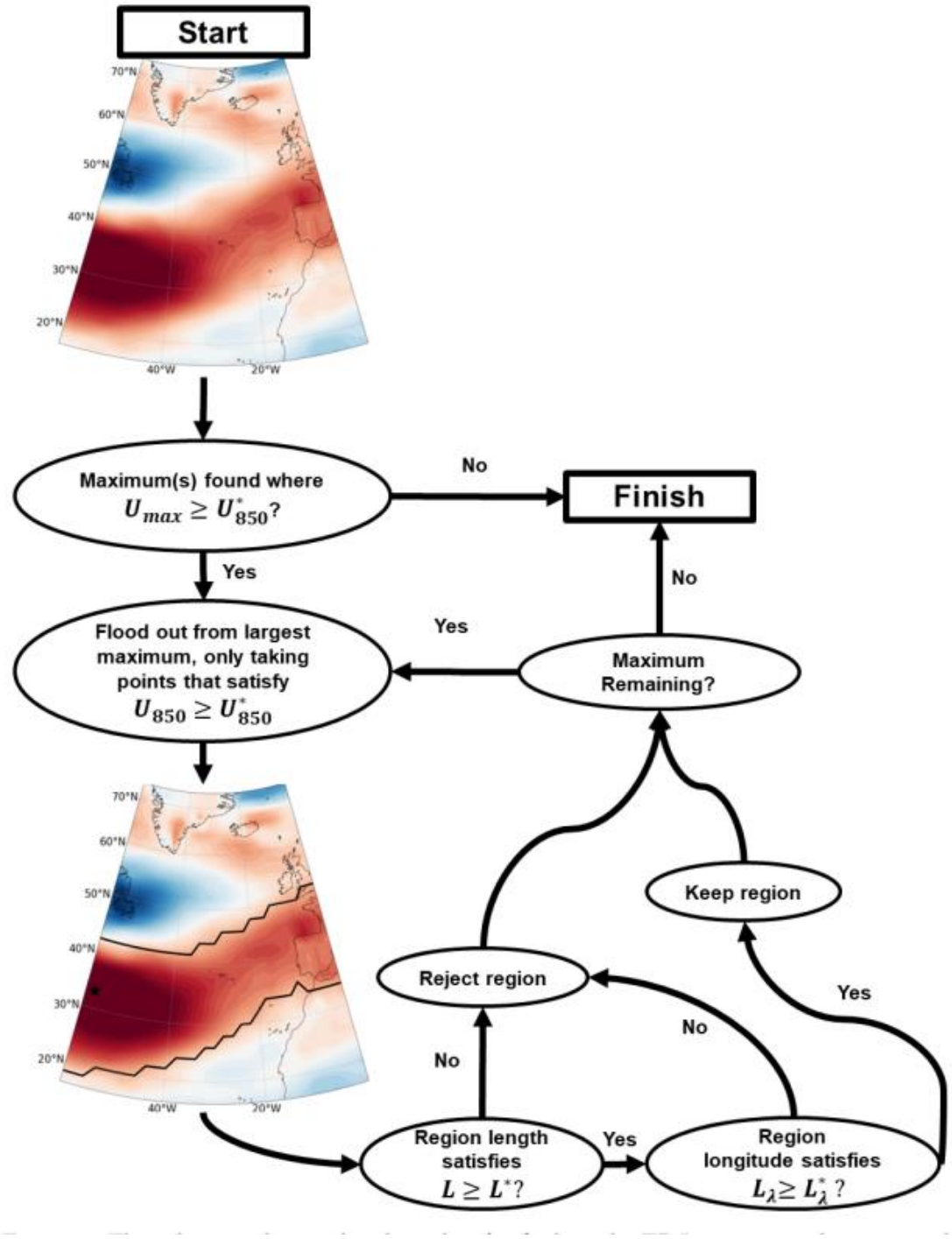

Figure A1. Flow chart outlining the algorithm for finding the NAJ regions, with an example day. Parameters used for thresholding are U^*_{850} (seed point and flooding threshold), L^* (region length threshold) and L^*_λ (zonal length threshold). This figure follows the description outlined in Section 3.3.1. The single maximum found here is indicated by the black star. Figure courtesy of Jacob Perez.

APPENDIX II. Python code

Obtaining the jet indices

```
#In this cell the data is loaded
data_filename1 =
'/badc/cmip6/data/CMIP6/CMIP/CCCma/CanESM5/historical/r1i1p1f1/day/ua/gn/la
test/ua_day_CanESM5_historical_r1i1p1f1_gn_19910101-20001231.nc'
data_filename2 =
'/badc/cmip6/data/CMIP6/CMIP/CCCma/CanESM5/historical/r1i1p1f1/day/ua/gn/la
test/ua_day_CanESM5_historical_r1i1p1f1_gn_20010101-20101231.nc'
data_filename3 =
'/badc/cmip6/data/CMIP6/CMIP/CCCma/CanESM5/historical/r1i1p1f1/day/ua/gn/la
test/ua_day_CanESM5_historical_r1i1p1f1_gn_20110101-20141231.nc'
gridarea_filename = 'gridarea.nc'

#Once the data is loaded it is constrained to the North Atlantic
U1 = iris.load_cube(data_filename1)
U2 = iris.load_cube(data_filename2)
U3 = iris.load_cube(data_filename3)

iris.util.equalise_attributes([U1,U2,U3])
cubes = iris.cube.CubeList([U1,U2,U3])
U = cubes.concatenate_cube()

gridareas = iris.load_cube(gridarea_filename)

lon_constraint,lat_constraint,level_constraint =
[300,360],[15,75],[85000,85000]
U = constrain_data(U,level_constraint,lat_constraint,lon_constraint)

add_season_membership(U, 'time', 'DJF', name='in_djf')
constraint = iris.Constraint(in_djf=True)
U_winter = U.extract(constraint)
add_season_year(U_winter, 'time', name='season_year',
seasons=['DJF','MAMJJASON'])

t_constraint = iris.Constraint(time=lambda cell: 1995 <= cell.point.year <=
2014)
U_winter = U_winter.extract(t_constraint)
gridareas = constrain_data(gridareas,None,lat_constraint,lon_constraint)

lon,lat = U.coord('longitude').points,U.coord('latitude').points

#This cell runs the EDJ region finding algorithm. The values here are the
thresholds that we have been using for our studies.
Ustar= 8
min_length = 1661
min_zonal_length = 20
regions_store,flood_store,region_maxima_coords =
blob_finder(U_winter,Ustar,gridareas,min_length,min_zonal_length)

#This cell finds the number of regions on each day and the index for the
regions with the largest mass
num_of_labels = []
N = len(U.data)
for i in range(0,N):
    num_of_labels.append(len(regions_store[i]))
```

```
largest_mass_regions = np.zeros(N,dtype=object)
largest_mass_flood = np.zeros(N,dtype=object)
largest_mass_maxima = np.zeros(N,dtype=object)

del_index_mass= []
max_index_store = []

for i in np.arange(0,N):
        mass_store = []
        if regions_store[i] == []:
                mass_store.append(0)
        else:
                for k,regions in enumerate(regions_store[i]):
                        region_edj =
                        EDJregion(regions[0],flood_store[i][k],U.data[i],gri
                        dareas,lon,lat)
                        mass_store.append(region_edj.mass())

                max_mass_index = np.argmax(mass_store)
                max_index_store.append(max_mass_index)

                largest_mass_regions[i] = regions_store[i][max_mass_index]
                largest_mass_flood[i] = flood_store[i][max_mass_index]

#This cell returns the jet diagnostics for the largest mass regions.
Umass_values= []
alpha_values = []
alpha_values = []
phibar_values = []
Umean_values = []

for i,region in enumerate(largest_mass_regions):
    if region == 0:
        Umass_values.append(0)
        alpha_values.append(0)
        phibar_values.append(0)
        Umean_values.append(0)
    else:
        region_edj =
        EDJregion(region[0],flood_store[i][k],U.data[i],gridareas,lon,lat)
        phibar_values.append(region_edj.phibar())
        alpha_values.append(region_edj.alpha())
        Umass_values.append(region_edj.mass())
        Umean_values.append(region_edj.mean_intensity())

Umass = np.array(Umass_values)
alpha = np.array(alpha_values)
phibar = np.array(phibar_values)
Umean = np.array(Umean_values)

#This cell saves the files.
np.save('phibar.npy',phibar)
np.save('Umass.npy',Umass)
np.save('alpha.npy',alpha)
np.save('Umean.npy',Umean)
```

Model evaluatio

```
import numpy as np
import matplotlib.pyplot as plt
import scipy.stats
import statistics
import pandas as pd
from scipy.stats import norm, kstest
from scipy.stats import describe
from scipy.stats import ks_2samp
import math
from statsmodels.tsa.stattools import acf
import scipy.stats as stats
def r(ts):
    lag_corr = []
    for i in range(0,len(ts)):
        vals = acf(ts[i])
        print(vals)
        lag_corr.append(vals[1])

    return np.mean(lag_corr)
def rtemp(ts):
    return acf(ts)[1]

def my_ks_2samp(s1,s2,alpha,r1,r2):

    # Gets all observations
    s1 = np.sort(s1)
    s2 = np.sort(s2)
    observations = np.concatenate([s1, s2])

    #generate cdfs
    m,n = len(s1),len(s2)
    cdf1 = np.searchsorted(s1, observations, side='right')/m
    cdf2 = np.searchsorted(s2, observations, side='right')/n

    #change smaple size to effective samaple size
    meff,neff= ((1-r1)/(1+r1))*m,((1-r2)/(1+r2))*n
    en = meff * neff / (meff + neff)

    #compute statistic for given confidence interval
    C =np.sqrt(-np.log(alpha/2)*0.5)
    A = C*np.sqrt(1/en)

    #take difference between cdfs
    cddiffs = cdf1 - cdf2
    argminS = np.argmin(cddiffs)
    argmaxS = np.argmax(cddiffs)

    # Ensure sign of minS is not negative.
    minS = np.clip(-cddiffs[argminS], 0, 1)
    maxS = cddiffs[argmaxS]

    if  minS > maxS:
        d = minS
    else:
        d = maxS

    p_value = stats.kstwo.sf(d, np.round(en))
```

```
    return {"statistic": d, "pvalue" : p_value, "c_value": A}

variable = 'phibar'
modelname1 = 'IPSL-CM6A-LR'
modelname2 = 'CNRM-CM6-1'
modelname3 = 'UKESM1-0-LL'
modelname4 = 'CanESM5'
modelname6 = 'ACCESS-ESM1-5'

model1 = np.load(''+variable+'_'+modelname1+'_historical.npy')
model2 = np.load(''+variable+'_'+modelname2+'_historical.npy')
model3 = np.load(''+variable+'_'+modelname3+'_historical.npy')
model4 = np.load(''+variable+'_'+modelname4+'_historical.npy')
model6 = np.load(''+variable+'_'+modelname6+'_historical.npy')

ERA5 = np.load('ERA5_'+variable+'.npy')

if(variable=='phibar'):
    binvals=np.arange(25,75,1)
    units='[deg N]'
if(variable=='alpha'):
    binvals=np.arange(-60,60,2)
    units='[deg]'
if(variable=='Umean'):
    binvals=np.arange(7.5,22.5,0.6)
    units='[m/s]'
if(variable=='Umass'):
    binvals=np.arange(0,3,0.05)
    units='[1E14 km^2 m/s]'
    ERA5=ERA5/1E14

#CALCULATE K-S TEST
#model1
r1 = rtemp(model1)
r5 = rtemp(ERA5)

KS1 = my_ks_2samp(model1,ERA5,0.05,r1,r5)
print(KS1)

statistic = "{:.2e}".format(KS1["statistic"])
pvalue = "{:.2e}".format(KS1["pvalue"])

#model2
r2 = rtemp(model2)

KS2 = my_ks_2samp(model2,ERA5,0.05,r2,r5)
print(KS2)

statistic2 = "{:.2e}".format(KS2["statistic"])
pvalue2 = "{:.2e}".format(KS2["pvalue"])

#model3
r3 = rtemp(model3)

KS3 = my_ks_2samp(model3,ERA5,0.05,r3,r5)
```

```
print(KS3)
statistic3 = "{:.2e}".format(KS3["statistic"])
pvalue3 = "{:.2e}".format(KS3["pvalue"])

#model4
r4 = rtemp(model4)

KS4 = my_ks_2samp(model4,ERA5,0.05,r4,r5)
print(KS4)
statistic4 = "{:.2e}".format(KS4["statistic"])
pvalue4 = "{:.2e}".format(KS4["pvalue"])

#model6
r6 = rtemp(model6)

KS6 = my_ks_2samp(model6,ERA5,0.05,r6,r5)
print(KS6)
statistic6 = "{:.2e}".format(KS6["statistic"])
pvalue6 = "{:.2e}".format(KS6["pvalue"])

plt.hist(model1, density=True, bins = binvals, histtype='step',
stacked=True, fill=False, color='blue', label= modelname1)
plt.hist(model2, density=True, bins = binvals, histtype='step',
stacked=True, fill=False, color='orange', label= modelname2)
plt.hist(model3, density=True, bins = binvals, histtype='step',
stacked=True, fill=False, color='green', label= modelname3)
plt.hist(model4, density=True, bins = binvals, histtype='step',
stacked=True, fill=False, color='red', label= modelname4)
plt.hist(model6, density=True, bins = binvals, histtype='step',
stacked=True, fill=False, color='purple', label= modelname6)
plt.hist(ERA5, density=True, bins = binvals, histtype='step', stacked=True,
fill=False, color='black', label= 'ERA5')
plt.ylabel('Density')
plt.xlabel(variable+' '+units)
plt.title('Daily mean present day data comparison between models (1995-
2014)')
plt.legend()
plt.savefig("test.png")


pd.DataFrame({modelname1: [(round(statistics.median(model1),2)),
(round(statistics.mean(model1),2)), (round(statistics.stdev(model1), 2)),
(round(scipy.stats.skew(model1),2))],
              modelname2: [(round(statistics.median(model2),2)),
(round(statistics.mean(model2),2)), (round(statistics.stdev(model2),2)),
(round(scipy.stats.skew(model2),2))],
             modelname3: [(round(statistics.median(model3),2)),
(round(statistics.mean(model3),2)),
(round(statistics.stdev(model3),2)),(round(scipy.stats.skew(model3),2)),],
              modelname4: [(round(statistics.median(model4),2)),
(round(statistics.mean(model4),2)),
(round(statistics.stdev(model4),2)),(round(scipy.stats.skew(model4),2)),],
              modelname6: [(round(statistics.median(model6),2)),
(round(statistics.mean(model6),2)),
(round(statistics.stdev(model6),2)),(round(scipy.stats.skew(model6),2)),],
```

```
'ERA5': [(round(statistics.median(ERA5),2)),
(round(statistics.mean(ERA5),2)),
(round(statistics.stdev(ERA5),2)),(round(scipy.stats.skew(ERA5),2)),]},
             index=['Median', 'Mean', 'Standard Deviation', 'Skweness'])

pd.DataFrame({modelname1+' and ERA5': [statistic+', '+pvalue],
              modelname2+' and ERA5': [statistic2+', '+pvalue2],
              modelname3+' and ERA5': [statistic3+', '+pvalue3],
              modelname4+' and ERA5': [statistic4+', '+pvalue4],
             modelname6+' and ERA5': [statistic6+', '+pvalue6],},
             index=['K-S test (statistic, p-value)'])
```

Future projections of the NAJ under SSP3-7.0

```
import numpy as np
import matplotlib.pyplot as plt
import scipy.stats
import statistics
import pandas as pd
from scipy.stats import norm, kstest
from scipy.stats import describe
from scipy.stats import ks_2samp
import math
from statsmodels.tsa.stattools import acf
import scipy.stats as stats
from matplotlib.legend import Legend
from math import sqrt
from numpy.random import seed
from numpy.random import randn
from numpy import mean
from scipy.stats import sem
from scipy.stats import t

def r(ts):
    lag_corr = []
    for i in range(0,len(ts)):
        vals = acf(ts[i])
        print(vals)
        lag_corr.append(vals[1])

    return np.mean(lag_corr)
def rtemp(ts):
    return acf(ts)[1]

def my_ks_2samp(s1,s2,alpha,r1,r2):

    # Gets all observations
    s1 = np.sort(s1)
    s2 = np.sort(s2)
    observations = np.concatenate([s1, s2])

    #generate cdfs
    m,n = len(s1),len(s2)
    cdf1 = np.searchsorted(s1, observations, side='right')/m
    cdf2 = np.searchsorted(s2, observations, side='right')/n

    #change smaple size to effective samaple size
    meff,neff= ((1-r1)/(1+r1))*m,((1-r2)/(1+r2))*n
    en = meff * neff / (meff + neff)

    #compute statistic for given confidence interval
    C =np.sqrt(-np.log(alpha/2)*0.5)
    A = C*np.sqrt(1/en)

    #take difference between cdfs
    cddiffs = cdf1 - cdf2
    argminS = np.argmin(cddiffs)
    argmaxS = np.argmax(cddiffs)

    # Ensure sign of minS is not negative.
    minS = np.clip(-cddiffs[argminS], 0, 1)
```

```
    maxS = cddiffs[argmaxS]

    if  minS > maxS:
        d = minS
    else:
        d = maxS

    p_value = stats.kstwo.sf(d, np.round(en))
    return {"statistic": d, "pvalue" : p_value, "c_value": A}

variable = 'Umass'
modelname = 'ACCESS-ESM1-5'


if(variable=='phibar'):
    binvals=np.arange(25,76,1)
    units='[deg N]'
if(variable=='alpha'):
    binvals=np.arange(-60,60,2)
    units='[deg]'
if(variable=='Umean'):
    binvals=np.arange(7.5,22.5,0.6)
    units='[m/s]'
if(variable=='Umass'):
    binvals=np.arange(0,3,0.05)
    units='[1E14 km^2 m/s]'

if(modelname == 'IPSL-CM6A-LR'):
    nhist=10
    nfut=11
    fv='1'
    lletra= '(a)'
if(modelname == 'UKESM1-0-LL'):
    nhist=20
    nfut=20
    fv='2'
    lletra= '(b)'
if(modelname == 'CNRM-CM6-1'):
    nhist=10
    nfut=7
    fv='2'
    lletra= '(c)'
if(modelname == 'CanESM5'):
   nhist=8
   nfut=8
   fv='1'
   lletra= '(d)'
if(modelname == 'ACCESS-ESM1-5'):
    nhist=9
    nfut=9
    fv='1'
    lletra= '(e)'

for ens in np.arange(1,nhist,1):
    if(ens == 1):
```

```
        data =
np.load('/home/users/earjcas/data/diags/'+modelname+'/'+variable+'_'+modeln
ame+'_historical_r'+str(ens)+'i1p1f'+fv+'.npy')
        data = data[np.where(data != 0)]
    else:
        if(modelname =='IPSL-CM6A-LR' and ens == 7):
            print()
        else:
            if(modelname =='UKESM1-0-LL' and ens == 13 or ens == 14 or ens
==  15):
                print()
            else:
                dum =
np.load('/home/users/earjcas/data/diags/'+modelname+'/'+variable+'_'+modeln
ame+'_historical_r'+str(ens)+'i1p1f'+fv+'.npy')
                dum = dum[np.where(dum != 0)]
                data = np.concatenate((data,dum))

for ens in (np.arange(1,nfut,1)):
        if (ens == 1 and modelname != 'ACCESS-ESM1-5'):
            data2=
np.load('/home/users/earjcas/data/diags/'+modelname+'/'+variable+'_'+modeln
ame+'_ssp370_r'+str(ens)+'i1p1f'+fv+'.npy')
            data2 = data2[np.where(data2 !=0)]
        else:
            if(modelname =='IPSL-CM6A-LR' and ens == 7):
                print()
            else:
                if(modelname == 'UKESM1-0-LL' and ens == 13 or ens == 14 or
ens == 15):
                    print()
                else:
                    if(modelname =='ACCESS-ESM1-5' and ens==1):
                        print()
                    else:
                        if(modelname == 'ACCESS-ESM1-5' and ens == 2):
                            data2=
np.load('/home/users/earjcas/data/diags/'+modelname+'/'+variable+'_'+modeln
ame+'_ssp370_r'+str(ens)+'i1p1f'+fv+'.npy')
                            data2 = data2[np.where(data2 !=0)]
                        else:
                            dum =
np.load('/home/users/earjcas/data/diags/'+modelname+'/'+variable+'_'+modeln
ame+'_ssp370_r'+str(ens)+'i1p1f'+fv+'.npy')
                            dum = dum[np.where(dum != 0)]
                            data2 = np.concatenate((data2,dum))

if(variable=='Umass'):
    data=data/1E14
    data2=data2/1E14

#CALCULATE K-S TEST

r1 = rtemp(data)
r2 = rtemp(data2)

KS = my_ks_2samp(data,data2,0.05,r1,r2)
```

```
print(KS)

statistic = "{:.2e}".format(KS["statistic"])
pvalue = "{:.2e}".format(KS["pvalue"])
print("{:.2e}".format(KS["statistic"]))
print("{:.2e}".format(KS["pvalue"]))


#CALCULTATE T-STUDENT TEST FOR TWO INDEPENDENT SAMPLES

def independent_ttest(data, data2, alpha1):
 # calculate means
    mean1, mean2 = mean(data), mean(data2)
 # calculate standard errors
    se1, se2 = np.var(data), np.var(data2)
 # standard error on the difference between the samples
    sed = sqrt(se1**2.0 + se2**2.0)
 # calculate the t statistic

 # degrees of freedom
    m,n = len(data),len(data2)
    r1 = rtemp(data)
    r2 = rtemp(data2)
    print(r1,r2)
    meff,neff= ((1-r1)/(1+r1))*m,((1-r2)/(1+r2))*n
    #Neff = ((1-r1*r2)/(1+r2*r1))*max(m,n)
    df = meff+neff-2
    print(df)
    sp = np.sqrt(((meff-1)*se1**2 + (neff-1)*se2**2)/df)
    #sp = np.sqrt(sed/2)
    t_stat = (mean1 - mean2) / (sp*np.sqrt(1/meff + 1/neff))
    #t_stat = (mean1-mean2)/sp*np.sqrt(2/Neff)
 # calculate the critical value
    cv = t.ppf(1.0 - alpha1, df)
 # calculate the p-value
    #p = (1.0 - t.cdf(abs(t_stat), df)) * 2.0
    p = 2*t.sf(abs(t_stat),df)
 # return everything
    return t_stat, df, cv, p

# calculate the t test
alpha1 = 0.05
t_stat, df, cv, p = independent_ttest(data, data2, alpha1)
print('t=%.3f, df=%d, cv=%.3f, p=%.3f' % (t_stat, df, cv, p))
# interpret via critical value
if abs(t_stat) <= cv:
 print('Accept null hypothesis that the means are equal. The sample means
are equal')
else:
 print('Reject the null hypothesis that the means are equal. The sample
means are different')
# interpret via p-value
if p > alpha1:
 print('Accept null hypothesis that the means are equal.The sample means
are equal')
else:
```

```
print('Reject the null hypothesis that the means are equal. The sample
means are different')

#PLOT HISTOGRAM

plt.hist(data, density=True, bins=binvals, histtype='step', stacked=True,
fill=False, color='blue', label='1995-2014')  # density=False would make
counts
plt.hist(data2, density=True, bins=binvals, histtype='step', stacked=True,
fill=False, color='orange', label='2080-2099')  # density=False would make
counts
plt.ylabel('Density')
plt.xlabel(variable+' '+units)
plt.title(modelname)
plt.legend()

#pvalue = "{:.2f}".format(KS["pvalue"])
print(pvalue)
#PLOT DATA FRAME

pd.DataFrame({'1995-2014': [statistics.median(data), statistics.mean(data),
statistics.stdev(data),scipy.stats.skew(data),statistic+', '+pvalue],
              '2080-2099': [statistics.median(data2),
statistics.mean(data2), statistics.stdev(data2),scipy.stats.skew(data2),
statistic+', '+pvalue]},
             index=['Median', 'Mean', 'Standard Deviation', 'Skweness', 'K-
S test (statistic, p-value)'])

#PLOT T-STUDENT DATA FRAME
pd.DataFrame({"Mean Student's t-Test": [t_stat, df, cv, p]},
             index= ['t statistic', 'degrees of freedom', 'critical value',
'p-value'])

fig, ax = plt.subplots()

ax.hist(data, density=True, bins=binvals, histtype='step', stacked=True,
fill=False, color='blue', label='1995-2014')
ax.hist(data2, density=True, bins=binvals, histtype='step', stacked=True,
fill=False, color='orange', label='2080-2099')
ax.set_ylabel('Density')
ax.set_xlabel(variable+' '+units)
ax.set_title(modelname)
ax.legend(loc = "upper right")

font = {'family': 'sans-serif',
        'color':  'black',
        'weight': 'normal',
        'size': 10,
        }
fontbold = {'family': 'sans-serif',
        'color':  'black',
        'weight': 'bold',
        'size': 10,
        }
mean_present =   str(round(statistics.mean(data),2))
mean_future =   str(round(statistics.mean(data2),2))
sd_present =  str(round(statistics.stdev(data),2))
```

```
sd_future =  str(round(statistics.stdev(data2),2))
skew_present =  str(round(scipy.stats.skew(data),2))
skew_future =  str(round(scipy.stats.skew(data2),2))
#pvalue = str(round(KS["pvalue"],3))
pvalue = pvalue = "{:.2e}".format(KS["pvalue"])
print(p)
print(pvalue)

if p <  0.05:
    ax.text(0.70, 0.75, 'μ: ['+ mean_present+', '+mean_future+']',
fontdict=fontbold,transform=ax.transAxes) #2.2, 1
    ax.text(0.7, 0.65, 'σ: ['+ sd_present+', '+sd_future+']',
fontdict=font,transform=ax.transAxes)
    ax.text(0.7, 0.55, 'skew: ['+ skew_present+', '+skew_future+']',
fontdict=font,transform=ax.transAxes)
    ax.text(0.7, 0.45, 'p(K-S):'+ pvalue,
fontdict=font,transform=ax.transAxes)
    ax.text(0.01, 0.95,lletra, fontdict=fontbold,transform=ax.transAxes)
else:
    ax.text(0.03, 0.85, 'μ: ['+ mean_present+', '+mean_future+']',
fontdict=font,transform=ax.transAxes)#2.2, 1.05
    ax.text(0.03, 0.75, 'σ: ['+ sd_present+', '+sd_future+']',
fontdict=font,transform=ax.transAxes)
    ax.text(0.03, 0.65, 'skew: ['+ skew_present+', '+skew_future+']',
fontdict=font,transform=ax.transAxes)
    ax.text(0.03, 0.55, 'p(K-S):'+ pvalue,
fontdict=font,transform=ax.transAxes)
    ax.text(0.01, 0.95,lletra, fontdict=fontbold,transform=ax.transAxes)

plt.show()

np.save(''+variable+'_'+modelname+'_historical.npy', data)
np.save(''+variable+'_'+modelname+'_future.npy', data2)
```

Winter mean changes MAP

```
import cartopy
model = 'CanESM5'


if(model == 'UKESM-0-LL'):
    ens = [1,2,3,4,5,6,7,8,9,10,11,12,16,17,18,19]
if(model == 'CNRM-CM6-1'):
    ens = [1,2,3,4,5,6]
if(model == 'IPSL-CM6A-LR'):
    ens = np.arange(1,10,1)
if(model == 'CanESM5'):
    ens = [1,2,3,4,5,6,7]
if(model == 'ACCESS-ESM1-5'):
    ens = [2,3,4,5,6,7,8]
for ind in ens:

    print(ind)

    '''
    This cell loads your data, you will need to change the filenames for
your data.
    Once the data is loaded c
    '''
    if(model == 'UKESM-0-LL'):
        if(ind == 5 or ind == 6 or ind == 7):
            data_filename = f'/badc/cmip6/data/CMIP6/CMIP/MOHC/UKESM1-0-
LL/historical/r{ind}i1p1f3/Amon/ua/gn/latest/ua_Amon_UKESM1-0-
LL_historical_r{ind}i1p1f3_gn_195001-201412.nc'
        else:
            data_filename = f'/badc/cmip6/data/CMIP6/CMIP/MOHC/UKESM1-0-
LL/historical/r{ind}i1p1f2/Amon/ua/gn/latest/ua_Amon_UKESM1-0-
LL_historical_r{ind}i1p1f2_gn_195001-201412.nc'

    if(model == 'CNRM-CM6-1'):
        data_filename = f'/badc/cmip6/data/CMIP6/CMIP/CNRM-CERFACS/CNRM-
CM6-1/historical/r{ind}i1p1f2/Amon/ua/gr/latest/ua_Amon_CNRM-CM6-
1_historical_r{ind}i1p1f2_gr_185001-201412.nc'

    if(model == 'IPSL-CM6A-LR'):
        if(ind == 10):
            print()
        else:
            data_filename = f'/badc/cmip6/data/CMIP6/CMIP/IPSL/IPSL-CM6A-
LR/historical/r{ind}i1p1f1/Amon/ua/gr/latest/ua_Amon_IPSL-CM6A-
LR_historical_r{ind}i1p1f1_gr_185001-201412.nc'

    if(model == 'CanESM5'):
        data_filename =
f'/badc/cmip6/data/CMIP6/CMIP/CCCma/CanESM5/historical/r{ind}i1p1f1/Amon/ua
/gn/latest/ua_Amon_CanESM5_historical_r{ind}i1p1f1_gn_185001-201412.nc'

    if(model == 'ACCESS-ESM1-5'):
        if(ind == 1):
            print()
        else:
            data_filename = f'/home/users/earjcas/data/diags/ACCESS-ESM1-
5/Amon/ua_Amon_ACCESS-ESM1-5_historical_r{ind}i1p1f1_gn_195001-201412.nc'
```

```
    U = iris.load_cube(data_filename)


    U = U.extract(iris.Constraint(latitude=lambda cell: 15 <= cell <= 75))
    U = U.extract(iris.Constraint(longitude=lambda cell: 300 <= cell <=
360))
    U = U.extract(iris.Constraint(air_pressure=85000))

    add_season_membership(U, 'time', 'DJF', name='in_djf')
    constraint = iris.Constraint(in_djf=True)
    U_winter = U.extract(constraint)
    add_season_year(U_winter, 'time', name='season_year',
seasons=['DJF','MAMJJASON'])
    t_constraint = iris.Constraint(time=lambda cell: 1995 <=
cell.point.year <= 2014)
    U_hist_winter = U_winter.extract(t_constraint)
    U_hist_mean = U_winter.collapsed('time', iris.analysis.MEAN)
    lon,lat =
U_hist_mean.coord('longitude').points,U_hist_mean.coord('latitude').points

    if(model == 'UKESM-0-LL'):
        data_filename = f'/badc/cmip6/data/CMIP6/ScenarioMIP/MOHC/UKESM1-0-
LL/ssp370/r{ind}i1p1f2/Amon/ua/gn/latest/ua_Amon_UKESM1-0-
LL_ssp370_r{ind}i1p1f2_gn_205001-210012.nc'

    if(model == 'CNRM-CM6-1'):
        data_filename = f'/badc/cmip6/data/CMIP6/ScenarioMIP/CNRM-
CERFACS/CNRM-CM6-1/ssp370/r{ind}i1p1f2/Amon/ua/gr/latest/ua_Amon_CNRM-CM6-
1_ssp370_r{ind}i1p1f2_gr_201501-210012.nc'

    if(model == 'IPSL-CM6A-LR'):
        data_filename = f'/badc/cmip6/data/CMIP6/ScenarioMIP/IPSL/IPSL-
CM6A-LR/ssp370/r{ind}i1p1f1/Amon/ua/gr/latest/ua_Amon_IPSL-CM6A-
LR_ssp370_r{ind}i1p1f1_gr_201501-210012.nc'
    if(model == 'CanESM5'):
        data_filename =
f'/badc/cmip6/data/CMIP6/ScenarioMIP/CCCma/CanESM5/ssp370/r{ind}i1p1f1/Amon
/ua/gn/latest/ua_Amon_CanESM5_ssp370_r{ind}i1p1f1_gn_201501-210012.nc'
    if(model == 'ACCESS-ESM1-5'):
        data_filename = f'/home/users/earjcas/data/diags/ACCESS-ESM1-
5/Amon/ua_Amon_ACCESS-ESM1-5_ssp370_r{ind}i1p1f1_gn_201501-210012.nc'


    U = iris.load_cube(data_filename)
    U = U.extract(iris.Constraint(latitude=lambda cell: 15 <= cell <= 75))
    U = U.extract(iris.Constraint(longitude=lambda cell: 300 <= cell <=
360))
    U = U.extract(iris.Constraint(air_pressure=85000))

    add_season_membership(U, 'time', 'DJF', name='in_djf')
    constraint = iris.Constraint(in_djf=True)
    U_winter = U.extract(constraint)
    add_season_year(U_winter, 'time', name='season_year',
seasons=['DJF','MAMJJASON'])
    t_constraint = iris.Constraint(time=lambda cell: 2080 <=
cell.point.year <= 2099)
```

```
    U_fut_winter = U_winter.extract(t_constraint)
    U_fut_mean = U_winter.collapsed('time', iris.analysis.MEAN)

    if(ind == 1 and model != 'ACCESS-ESM1-5'):
        Udiff = U_fut_winter.data - U_hist_winter.data
        Uclim = U_hist_winter.data
    else:
        if(model == 'ACCESS-ESM1-5' and ind == 1):
             print()
        else:
            if(model == 'ACCESS-ESM1-5' and ind==2):
                Udiff = U_fut_winter.data - U_hist_winter.data
                Uclim = U_hist_winter.data
            else:
                Udum = U_fut_winter.data - U_hist_winter.data
                Udiff = np.concatenate((Udiff,Udum))
                Udum = U_hist_winter.data
                Uclim = np.concatenate((Uclim,Udum))

Udiff = np.mean(Udiff,axis=0)
Udiff = np.where(Udiff > 500, np.nan, Udiff)
Uclim = np.mean(Uclim,axis=0)
Uclim = np.where(Uclim > 500, np.nan, Uclim)

np.save(''+model+'_map.npy', Udiff)
np.save(''+model+'_clim.npy', Uclim)
```

Plotting the maps

```
import matplotlib.pyplot as plt
import cartopy
import cartopy.crs as ccrs
import matplotlib.pyplot as plt
import numpy as np
model1 = np.load('CNRM-CM6-1_map.npy')
model1clim = np.load('CNRM-CM6-1_clim.npy')
model2 = np.load('IPSL-CM6A-LR_map.npy')
model2clim = np.load('IPSL-CM6A-LR_clim.npy')
model3 = np.load('UKESM-0-LL_map.npy')
model3clim = np.load('UKESM-0-LL_clim.npy')
model4 = np.load('CanESM5_map.npy')
model4clim = np.load('CanESM5_clim.npy')
model6 = np.load('ACCESS-ESM1-5_map.npy')
model6clim = np.load('ACCESS-ESM1-5_clim.npy')

fig, axs = plt.subplots(nrows=1,ncols=5,
                        subplot_kw={'projection': ccrs.PlateCarree()},
                        figsize=(18,8.5))
axs=axs.flatten()
clevels = np.linspace(-2.5,2.5,21)
clevels_clim = np.linspace(0,25,5)
cs = axs[0].contourf(model1,  transform =
ccrs.PlateCarree(),cmap='RdBu_r',levels=clevels, extent=(-60,0,15,75),
origin="lower")
axs[0].contour(model1clim,  transform =
ccrs.PlateCarree(),colors=['black'], levels=clevels_clim, extent=(-
60,0,15,75), origin="lower")
axs[1].contourf(model2,  transform = ccrs.PlateCarree(),
cmap='RdBu_r',levels=clevels, extent=(-60,0,15,75), origin="lower")
axs[1].contour(model2clim,  transform = ccrs.PlateCarree(),
colors=['black'],levels=clevels_clim, extent=(-60,0,15,75), origin="lower")
axs[2].contourf(model3, transform = ccrs.PlateCarree(),cmap='RdBu_r',
levels=clevels,extent=(-60,0,15,75), origin="lower")
axs[2].contour(model3clim,  transform =
ccrs.PlateCarree(),colors=['black'], levels=clevels_clim, extent=(-
60,0,15,75), origin="lower")
axs[3].contourf(model4, transform = ccrs.PlateCarree(),cmap='RdBu_r',
levels=clevels,extent=(-60,0,15,75), origin="lower")
axs[3].contour(model4clim,  transform =
ccrs.PlateCarree(),colors=['black'], levels=clevels_clim, extent=(-
60,0,15,75), origin="lower")
axs[4].contourf(model6, transform = ccrs.PlateCarree(),cmap='RdBu_r',
levels=clevels,extent=(-60,0,15,75), origin="lower")
axs[4].contour(model6clim,  transform =
ccrs.PlateCarree(),colors=['black'], levels=clevels_clim, extent=(-
60,0,15,75), origin="lower")

axs[0].coastlines(resolution="50m")
axs[1].coastlines(resolution="50m")
axs[2].coastlines(resolution="50m")
axs[3].coastlines(resolution="50m")
axs[4].coastlines(resolution="50m")

axs[0].set_title('CNRM-CM6-1', fontsize= 18)
axs[1].set_title('IPSL-CM6A-LR', fontsize= 18)
axs[2].set_title('UKESM1-0-LL', fontsize= 18)
```

```
axs[3].set_title('CanESM5', fontsize= 18)
axs[4].set_title('ACCESS-ESM1-5', fontsize= 18)

ax.text(0.01, 0.95,lletra, fontdict=fontbold)

cbar_ax = fig.add_axes([0.2, 0.45, 0.6, 0.02])
cbar=fig.colorbar(cs, cax=cbar_ax,orientation='horizontal',label="m/s")
plt.suptitle('Winter mean difference in 850hpa wind between 2080-99 and
1995-2014',fontsize=24)

fig.subplots_adjust(bottom=0.01, top=1.4, left=0.05, right=0.95,
                    wspace=0.1, hspace=0.1)

plt.show()
```